Chapter 12
Magnetoelastic Waves in Thin Films

Frederic Vanderveken, Florin Ciubotaru, and Christoph Adelmann

Abstract This chapter discusses the physics of magnetoelasticity and magnetoelastic waves in thin films as well as their mathematical description. Magnetoelastic waves occur as a result of strong coupling between spin waves and elastic waves in magnetostrictive ferromagnetic media. In a first part, the basic behavior of spin waves is reviewed in both bulk ferromagnets as well as in thin films. Next, elastic waves are discussed with a focus on thin films. Then, the interactions between the elastic and magnetic domains are described and it is shown how this results in the formation of magnetoelastic waves. The description and the mathematical formalism of magnetoelastic waves in infinitesimally thin films is extended to magnetoelastic waves in thin films with finite thickness. The dispersion relations and eigenstates are derived and graphically visualised for such magnetoelastic waves. It is shown that the behavior strongly depends on the geometry of the system, especially on the polarization of the spin and elastic waves and the direction of the magnetization of the magnetostrictive ferromagnetic medium.

12.1 Introduction

The coupling between different physical properties of a system is of great interest for transducer elements. In recent years, the field of spintronics, which includes applications of magnetism and magnetic materials in electronics, has gained enor-

F. Vanderveken
Departement Materiaalkunde, KU Leuven, 3001 Leuven, Belgium

F. Vanderveken (✉) · F. Ciubotaru · C. Adelmann
Imec, 3001 Leuven, Belgium
e-mail: Frederic.Vanderveken@imec.be

F. Ciubotaru
e-mail: Florin.Ciubotaru@imec.be

C. Adelmann
e-mail: Christoph.Adelmann@imec.be

E. Kamenetskii (ed.), *Chirality, Magnetism and Magnetoelectricity*,
Topics in Applied Physics 138,
https://doi.org/10.1007/978-3-030-62844-4_12

mous attention, which has led to the introduction of commercial magnetic memory technologies. However, the efficient energy conversion from the electric to the magnetic domain and vice versa still remains challenging. Current magnetic memories are based on spin-transfer or spin-orbit torques to switch the magnetization [1, 2]; however, these mechanisms depend on the current density in the device and require typically energies on the order of (10 s of) femtojoules to reverse the magnetization of a nanomagnet, despite a much lower intrinsic energy barrier of the order of attojoules. While femtojoule switching energies are promising for nonvolatile memories, they are not competitive in other spintronic applications, such as spintronic logic circuits. Therefore, much research has been devoted to developing more efficient transducers between electric and magnetic subsystems of spintronic devices.

One of the most promising devices to efficiently couple electric and magnetic properties in a spintronic system is the magnetoelectric transducer. Magnetoelectric transducers consist of composite materials, which comprise piezoelectric and magnetostrictive layers [3–7]. Applying a voltage to the piezoelectric layer(s) leads to the formation of strain in the compound. This strain introduces an effective magnetic anisotropy field in the magnetostrictive ferromagnetic component, leading to an coupling between voltage (electric field) and magnetization. The coupling is bidirectional since rotating the magnetization of a magnetostrictive layer also induces strain in the compound and consequently a polarization in the piezoelectric. Hence, such magnetoelectric schemes provide indirect coupling between electricity and magnetism mediated by elastodynamics. Since generating large electric fields in the piezoelectric layers can be energy efficiency, capacitive magnetoelectric transducers promise a much higher energy efficiency than their current-based counterparts.

The coupling scheme of a magnetoelectric transducer can be split into two parts, (i) piezoelectric coupling between electric and elastic domains, and (ii) magnetostrictive coupling between elastic and magnetic domains. Here, we investigate the second part and focus especially on the behavior at GHz frequencies that are relevant for fast electronic devices. In this frequency range, elastic waves (hypersound) interact with magnetic waves (spin waves), forming hybrid magnetoelastic waves under resonant conditions. The physics of the magnetoelastic resonance and the resulting magnetoelastic waves have been described in bulk and infinitesimally thin films decades ago [8–17]. However, modern applications of magnetoelastic waves in magnetoelectric and spintronic devices are based on nm-thick films. The finite thickness of these magnetic films alters the dynamic dipolar field with respect to infinitesimally thin films. Consequently, also the magnetoelastic coupling and the behavior of the magnetoelastic waves change due to the finite film thickness. In this chapter, the magnetoelastic theory and equations are extended to describe magnetoelastic waves in thin films of finite thickness.

The chapter begins by introducing basic magnetic interactions and by reviewing the properties of spin waves in bulk and thin film ferromagnets. The waves are described by a general formalism to calculate the eigensystem. The effect of the finite film thickness is then incorporated in this formalism. In the second part, linear elasticity and elastic waves in thin films are discussed. In the third part, the magnetoelastic interactions together with the combination of the magnetodynamic and

elastodynamic equations of motion are described. Finally, the fundamental properties of magnetoelastic waves in thin films with finite thickness are derived and illustrated both analytically and graphically for different magnetization orientations.

12.2 Spin Waves

Spin waves are collective excitations of the magnetization in magnetic materials. The properties of spin waves are strongly affected by the geometry and the dominant interactions inside the material. Hence, the relevant magnetic interactions will be shortly introduced, followed by the derivation of the properties of spin waves in bulk and thin film ferromagnets using the plane wave method.

12.2.1 Magnetic Interactions and Magnetization Dynamics

The magnetization dynamics in a ferromagnet can be described by the Landau–Lifshitz–Gilbert (LLG) equation [18, 19]

$$\frac{d\mathbf{M}}{dt} = -\gamma\mu_0(\mathbf{M}\times\mathbf{H}_{\text{eff}}) + \frac{\alpha}{M_\text{s}}\left(\mathbf{M}\times\frac{d\mathbf{M}}{dt}\right) \tag{12.1}$$

with γ the absolute value of the gyromagnetic ratio ($\text{s}^{-1}\text{T}^{-1}$), μ_0 the vacuum permeability (TmA^{-1}), α the Gilbert damping constant, M_s the saturation magnetization (Am^{-1}), and H_{eff} the effective magnetic field (Am^{-1}). The first term in the LLG equation describes the precession of the magnetization around the effective magnetic field. The second term in the LLG equation leads to the damping of the magnetization precession towards the direction of the effective magnetic field.

Multiple magnetic interactions and effects exist that influence the magnetization dynamics such as the exchange interaction, dipolar interaction, magnetocrystalline effect, magnetoelastic effect, etc.. It is possible to derive a magnetic field that corresponds to every interaction via

$$\mathbf{H} = -\frac{1}{\mu_0}\frac{\delta U(\mathbf{M})}{\delta\mathbf{M}} \quad \text{and} \quad U(\mathbf{M}) = \int_V \mathcal{E}(\mathbf{M})dV \tag{12.2}$$

with $\mathcal{E}(\mathbf{M})$ the corresponding energy density of that interaction. The total effective magnetic field H_{eff}, which is governing the magnetization dynamics in the LLG equation, is given by the sum of all individual magnetic fields, including externally applied fields. Below, the dipolar and exchange interaction are explained in more detail since these lead to spin waves. Fully elaborated discussions of spin waves and their properties can be found in [16, 20, 21].

The dipolar interaction describes the direct interaction between magnetic dipoles. Following (12.2), the interaction can be represented by a dipolar magnetic field. This field is found by solving Maxwell's equations. For spin waves at GHz frequencies, the magnetostatic approximation is valid since the wavelengths of such spin waves are several orders of magnitude shorter than those of electromagnetic waves in vacuum at the same frequency, i.e. $k_0 \ll k_{sw}$ with k_0 the wavenumber of an electromagnetic wave in vacuum and k_{sw} the wavenumber of a spin wave. This approximation implies that the change in electric field over time, $\partial \mathbf{E}/\partial t$, has a negligible effect on the generation of the magnetic field. Assuming further that no free charges and no electrical currents are present inside the material, Maxwell's equations become

$$\nabla \cdot \mathbf{E} = 0 \tag{12.3}$$

$$\nabla \cdot \mathbf{B} = 0 \tag{12.4}$$

$$\nabla \times \mathbf{E} = -\frac{\partial \mathbf{B}}{\partial t} \tag{12.5}$$

$$\nabla \times \mathbf{H} = 0 \tag{12.6}$$

with $\mathbf{B} = \mu_0(\mathbf{H} + \mathbf{M})$ the magnetic induction (T). Hence, in the magnetostatic limit (as in the electrostatic limit), electric and magnetic fields are decoupled from each other. Equation (12.6) indicates that the curl of the magnetic field equals zero. This allows for the definition of a magnetic scalar potential ϕ as

$$\mathbf{H}_{dip} = -\nabla\phi\,. \tag{12.7}$$

Using (12.4), the definition of the magnetic scalar potential and the magnetic induction $\mathbf{B}$, one finds the magnetic Poisson relation

$$\nabla^2\phi = \nabla \cdot \mathbf{M}\,. \tag{12.8}$$

This relation indicates that the divergence of the magnetization $\nabla \cdot \mathbf{M}$, also called the magnetic charge, acts as a source of the magnetic scalar potential and hence as a source of the dipolar field. Two types of magnetic charges can be identified: first, a surface charge, originating from surfaces between two materials with different magnetization magnitude or direction. Secondly, a magnetic volume charge, originating from the change of the magnetization in the bulk of a ferromagnetic material. Both surface and volume magnetic charges generate dipolar fields. The field outside the magnetic material is called the stray field and the field inside the material is called the demagnetization field.

By solving the magnetic Poisson equation (12.8) and using (12.7), it is possible to derive a general expression for the demagnetization field given by [22, 23]

$$\mathbf{H}_{demag} = \frac{1}{4\pi}\int_{V'} \bar{D}(\mathbf{r} - \mathbf{r}')\mathbf{M}(\mathbf{r}')dV' \tag{12.9}$$

with V' the volume of the magnetic material and $\bar{D}(\mathbf{r}-\mathbf{r}')$ the tensorial magnetostatic Green's function given by [16]

$$\bar{D}(\mathbf{r}-\mathbf{r}') = -\nabla_{\mathbf{r}}\nabla_{\mathbf{r}'}\frac{1}{|\mathbf{r}-\mathbf{r}'|}\,. \tag{12.10}$$

For uniform magnetization, the demagnetizing field is only generated by surface charges, and (12.9) reduces to

$$\mathbf{H}_{\text{demag}} = \frac{1}{4\pi}\mathbf{M}\int_{V'}\bar{D}(\mathbf{r}-\mathbf{r}')dV' = -\bar{N}(\mathbf{r})\mathbf{M} \tag{12.11}$$

with $\bar{N}(\mathbf{r})$ the demagnetization tensor, which only depends on the shape of the magnetic volume. The anisotropy introduced by the demagnetization field is thus often called the shape anisotropy.

The second magnetic interaction necessary to describe spin waves is the exchange interaction between individual magnetic dipoles. This interaction gives rise to ferromagnetic coupling below the Curie temperature [24]. The exchange energy density is given by

$$\mathcal{E}_{\text{ex}} = \frac{A_{\text{ex}}}{M_{\text{s}}^2}\left[(\nabla M_{\text{x}})^2 + (\nabla M_{\text{y}})^2 + (\nabla M_{\text{z}})^2\right] \tag{12.12}$$

with A_{ex} the exchange stiffness constant (J/m). Following (12.2), the exchange field is

$$\mathbf{H}_{\text{ex}} = \frac{2A_{\text{ex}}}{\mu_0 M_{\text{s}}^2}\Delta\mathbf{M} = l_{\text{ex}}^2\Delta\mathbf{M} \equiv \lambda_{\text{ex}}\Delta\mathbf{M} \tag{12.13}$$

with Δ the Laplace operator and l_{ex} the exchange length (m). In ferromagnets, the exchange interaction tries to keep the individual magnetic moments parallel. The exchange length l_{ex} characterizes the competition between the dipolar and the exchange interaction [21, 25]. At length scales below the exchange length l_{ex}, the exchange interaction is dominant and magnetic moments align parallel with each other. At length scales above the exchange length, the dipolar interaction is dominant, and it becomes possible for domains to form. Analogously, the properties of spin waves with short wavelengths are dominated by the exchange interaction, whereas the dipolar interaction strongly affects the properties of spin waves with large wavelengths.

12.2.2 Spin Waves in the Bulk Ferromagnets

Consider a ferromagnetic material with static magnetic field $\mathbf{H}_{\text{ext}}$ applied in the z-direction. In absence of any anisotropy, the external field forces the equilibrium magnetization along the z-direction. In such a system, stable wave-like excitations exist, which can be described by weak perturbations of the equilibrium magnetization. For a plane wave, the magnetization at a specific point in space and time can be written as

$$\mathbf{M}(\mathbf{r},t) = \mathbf{M}_0 + \mathbf{m}(\mathbf{r},t) = \begin{bmatrix} 0 \\ 0 \\ M_0 \end{bmatrix} + \begin{bmatrix} m_\text{x} \\ m_\text{y} \\ 0 \end{bmatrix} e^{i(\omega t + \mathbf{k}\cdot\mathbf{r})} \tag{12.14}$$

with ω the angular frequency of the wave (rad s^{-1}), and $\mathbf{k}$ the wavevector with norm $||\mathbf{k}|| = k = 2\pi/\lambda$ (rad m^{-1}) and direction perpendicular to the phase front. For weak perturbations, i.e. $||\mathbf{m}|| \ll M_0$, $\mathbf{m}(\mathbf{r},t)$ describes a wave-like perturbation which is called a spin wave.

In (12.14), the z-component of the dynamic magnetization, m_z, is neglected. This approximation is only valid if the perturbations are weak. Since the angular momentum, *i.e.* the norm of the magnetization vector, is conserved, the z-component is given by $m_\text{z}^2 = M_0^2 - m_\text{x}^2 - m_\text{y}^2$. Therefore, the m_z component can be considered as a second order perturbation and is neglected in the remainder of this chapter.

For a uniform bulk material, the dipolar and exchange fields that correspond to the perturbed magnetization state can be found via (12.9) and (12.13), respectively, and are given by [26]

$$\mathbf{h}_{\text{dip}}(\mathbf{r},t) = -\frac{\mathbf{k}\cdot\mathbf{m}(\mathbf{r},t)}{||\mathbf{k}||^2}\mathbf{k} = -\frac{1}{k^2}\begin{bmatrix} k_\text{x}^2 & k_\text{x}k_\text{y} & 0 \\ k_\text{x}k_\text{y} & k_\text{y}^2 & 0 \\ 0 & 0 & 0 \end{bmatrix}\mathbf{m}(\mathbf{r},t) \tag{12.15}$$

and

$$\mathbf{h}_{\text{ex}}(\mathbf{r},t) = -\lambda_{\text{ex}}k^2\mathbf{m}(\mathbf{r},t)\,. \tag{12.16}$$

The wavevector $\mathbf{k} = [k_x, k_y, k_z]$ is determined by a single parameter θ because of the axial symmetry around the magnetization vector. Hence, the wavevector can be written as $\mathbf{k} = k[\sin(\theta), 0, \cos(\theta)]$ with θ the angle between the magnetization and the propagation direction of the wave. With this substitution, the dipolar field can be simplified to

$$\mathbf{h}_{\text{dip}}(\mathbf{r},t) = -\begin{bmatrix} \sin^2(\theta) & 0 & 0 \\ 0 & 0 & 0 \\ 0 & 0 & 0 \end{bmatrix}\mathbf{m}(\mathbf{r},t)\,. \tag{12.17}$$

The magnetization dynamics corresponding to the spin wave is found by solving the LLG equation (12.1) including the perturbation $\mathbf{m}(\mathbf{r},t)$. Neglecting the damping

term, the LLG equation becomes

$$\frac{d[\mathbf{M}_0 + \mathbf{m}(\mathbf{r}, t)]}{dt} = -\gamma_0[(\mathbf{M}_0 + \mathbf{m}(\mathbf{r}, t)) \times (\mathbf{H}_{\text{ext}} + \mathbf{h}_{\text{dip}}(\mathbf{r}, t) + \mathbf{h}_{\text{ex}}(\mathbf{r}, t))] \tag{12.18}$$

with $\gamma_0 = \gamma\mu_0$. Terms quadratic in $\mathbf{m}$ can be neglected because the perturbation is assumed to be weak, which results in the linearized LLG equation given by

$$i\omega\mathbf{m}(\mathbf{r}, \omega) = -\gamma_0[\mathbf{M}_0 \times (\mathbf{h}_{\text{ex}}(\mathbf{r}, \omega) + \mathbf{h}_{\text{dip}}(\mathbf{r}, \omega)) + \mathbf{m}(\mathbf{r}, \omega) \times \mathbf{H}_{\text{ext}}]\,. \tag{12.19}$$

Rearranging the terms and rewriting the system in matrix notation leads to

$$\begin{bmatrix} \omega_{\text{bx}} & -i\omega \\ i\omega & \omega_{\text{by}} \end{bmatrix} \begin{bmatrix} m_{\text{x}} \\ m_{\text{y}} \end{bmatrix} = 0 \tag{12.20}$$

with

$$\omega_{\text{bx}} = \omega_0 + \omega_{\text{M}}(\lambda_{\text{ex}}k^2 + \sin^2(\theta)) \tag{12.21}$$

$$\omega_{\text{by}} = \omega_0 + \omega_{\text{M}}\lambda_{\text{ex}}k^2 \tag{12.22}$$

$\omega_0 = \gamma_0 H_{\text{ext}}$, and $\omega_{\text{M}} = \gamma_0 M_{\text{s}}$. The parameters ω_{bx} and ω_{by} are related to the effective magnetic fields that interact with the x- and y-components of the dynamic magnetization, respectively.

The properties of the stable perturbations of the magnetization, i.e. the spin waves, can be extracted by analyzing the eigenvalues and corresponding eigenstates of (12.20). Equation (12.20) has nontrivial solutions only if its determinant is zero. This condition can be utilized to obtain the dispersion relations of the spin waves. Considering only positive frequencies, the spin wave angular frequency is given by

$$\omega = \sqrt{\omega_{\text{bx}}\omega_{\text{by}}} = \sqrt{(\omega_0 + \omega_{\text{M}}\lambda_{\text{ex}}k^2)[\omega_0 + \omega_{\text{M}}(\lambda_{\text{ex}}k^2 + \sin^2(\theta))]}\,. \tag{12.23}$$

This equation is the dispersion relation for spin waves in bulk ferromagnets. It is also called the Herring–Kittel equation.

Equation (12.23) indicates that there is a nonzero minimum frequency, above which resonant magnetization dynamics are obtained. Exciting a ferromagnet at frequencies below the spin wave resonance generates evanescent waves. If the excitation source is removed, these waves disappear after a certain time (their lifetime) even in absence of intrinsic damping. Moreover, they do not propagate and thus do not contribute to steady state wave patterns at distances from the excitation source that are much larger than their wavelength. However, they are important to satisfy boundary conditions and in transient regimes.

The eigenstates corresponding to the eigenvalues of the linearized LLG equation are

$$\mathbf{m}(k) = \frac{N}{\sqrt{\omega_{\mathrm{bx}}\omega_{\mathrm{by}}}} \begin{bmatrix} i\omega_{\mathrm{by}} \\ \sqrt{\omega_{\mathrm{bx}}\omega_{\mathrm{by}}} \end{bmatrix} \tag{12.24}$$

with N a normalization constant. Note that ω_{bx} and ω_{by} both depend on k and thus, via the dispersion relation, also on the frequency. The eigenstate indicates that the precession of the magnetization (the polarization of the wave) is always clockwise in the direction of propagation. Furthermore, the precession of the magnetization is generally elliptical with an ellipticity equal to

$$\epsilon_{\mathrm{b}} = \frac{|m_{\mathrm{x}}|}{|m_{\mathrm{y}}|} = \frac{\omega_{\mathrm{by}}}{\sqrt{\omega_{\mathrm{bx}}\omega_{\mathrm{by}}}} \,. \tag{12.25}$$

In the limit of small k, the exchange interaction can be neglected since $\lambda_{\mathrm{ex}}k^2 \ll 1$, and the dispersion relation becomes $\omega = \sqrt{\omega_0(\omega_0 + \omega_{\mathrm{M}} \sin^2(\theta))}$. This dispersion relation characterizes dipolar spin waves that are degenerate. Hence, in this limit, multiple spin waves with different wavelengths exist at the same frequency. For $\theta = 0$, the dispersion relation becomes $\omega = \omega_0$ and the effect of the dipolar self-interaction disappears. In this case, the dynamic magnetization components only interact with the external field H_{ext}. For $\theta = \pi/2$, the interaction between the dynamic dipolar field and the spin wave is strongest. In this case, the dispersion relation is $\omega = \sqrt{\omega_0(\omega_0 + \omega_M)}$. Therefore, the spin wave frequencies in the dipolar regime are limited to a specific interval

$$\omega_0 \leq \omega \leq \sqrt{\omega_0(\omega_0 + \omega_M)} \,. \tag{12.26}$$

On the other hand, in the limit of large k, when $\lambda_{\mathrm{ex}}k^2 \gg 1$, a quadratic dispersion relation is obtained

$$\omega = \omega_{\mathrm{M}}\lambda_{\mathrm{ex}}k^2 \,. \tag{12.27}$$

This dispersion characterizes spin waves for which the exchange interaction is dominant. It is worth noting that these exchange spin waves are isotropic with respect to the propagation direction. By contrast, dipolar spin waves are anisotropic because they depend on the propagation direction via the parameter θ.

12.2.3 Spin Waves in Ferromagnetic Thin Films

In the previous section, the properties of spin waves in an infinite bulk medium were discussed. In this section, we introduce boundaries in the ferromagnetic medium and derive the properties of spin waves in ferromagnetic thin films of finite thickness.

Consider an infinite magnetic thin film of thickness d with its normal parallel to the y-direction. In the previous section, electrical currents were neglected in Maxwell's equations, which is only a good approximation for ferromagnetic insulators. How-

ever, for thin films, this approximation is even valid for conductors as long as the thickness of the film is sufficiently small with respect to the skin depth of the ferromagnet [27]. It should also be noted that in the derivations below, the dynamic magnetization and the fields are averaged over the thickness of the film and are thus uniform in the y-direction. This is a valid approximation when the wavelength is much larger than the thickness of the film, i.e. $kd \ll 1$. If this is not the case, it is possible for thickness modes to arise which have varying amplitude along the thickness [16]. These thickness modes will however not be considered here.

The magnetization is again defined as in (12.14) with the magnetization saturated in-plane along an external field $\mathbf{H}_{\text{ext}}$ in the z-direction. The components of the dynamic magnetization are in the x- and y-direction and form a plane wave, the spin wave. The exchange field is not affected by the thin film boundaries and is given by (12.13). As indicated by (12.8), the boundaries generate magnetic surface charges and therefore act as a source of the dipolar field. Therefore, in contrast with the exchange field, the dipolar field is affected by the boundaries.

For a thin film of finite thickness, the dipolar field can be approximated by [28–30]

$$\mathbf{h}_{\text{dip}}(\mathbf{r}, t) = -[P\frac{\mathbf{k}\cdot\mathbf{m}}{||\mathbf{k}||^2}\mathbf{k} + (1-P)(\mathbf{n}\cdot\mathbf{m})\mathbf{n}] \tag{12.28}$$

$$= -\begin{bmatrix} P\sin^2(\theta) & 0 & P\sin(\theta)\cos(\theta) \\ 0 & 1-P & 0 \\ P\sin(\theta)\cos(\theta) & 0 & P\cos^2(\theta) \end{bmatrix}\mathbf{m}(\mathbf{r}, t) \tag{12.29}$$

with

$$P = 1 - \frac{1-e^{-kd}}{kd}, \tag{12.30}$$

$k^2 = k_{\text{x}}^2 + k_{\text{z}}^2$, as well as θ the angle between the static magnetization $\mathbf{M}_0$ and wavevector $\mathbf{k}$. In the limit of an infinitesimally thin film, this simplifies to

$$\lim_{d\to 0}\mathbf{h}_{\text{dip}}(\mathbf{r}, t) = -\begin{bmatrix} 0 \\ 1 \\ 0 \end{bmatrix}\mathbf{m}(\mathbf{r}, t) \tag{12.31}$$

and thus only the out-of-plane magnetization component contributes to the spin wave dipolar field. Hence, for a thin film of finite thickness, the spin wave behavior is markedly different as compared to a thin film of infinitesimal thickness.

The linearized LLG equation (12.19) with the modified dipolar field in (12.28) can then be written as

$$\begin{bmatrix} \omega_{\text{fx}} & -i\omega \\ i\omega & \omega_{\text{fy}} \end{bmatrix}\begin{bmatrix} m_{\text{x}} \\ m_{\text{y}} \end{bmatrix} = 0 \tag{12.32}$$

with

$$\omega_{\mathrm{fx}} = \omega_0 + \omega_{\mathrm{M}}(\lambda_{\mathrm{ex}}k^2 + P\sin^2(\theta)) \tag{12.33}$$

$$\omega_{\mathrm{fy}} = \omega_0 + \omega_{\mathrm{M}}(\lambda_{\mathrm{ex}}k^2 + 1 - P)\,. \tag{12.34}$$

Again, nontrivial solutions of this equation only exist when the determinant of the matrix is zero. This condition leads to the dispersion relation of spin waves in thin ferromagnetic films, given by [30, 31]

$$\omega = \sqrt{\omega_{\mathrm{fx}}\omega_{\mathrm{fy}}} = \sqrt{(\omega_0 + \omega_{\mathrm{M}}\lambda_{\mathrm{ex}}k^2)(\omega_0 + \omega_{\mathrm{M}}\lambda_{\mathrm{ex}}k^2 + \omega_{\mathrm{M}}F_{\mathrm{m}})} \tag{12.35}$$

with

$$F_{\mathrm{m}} = 1 - P\cos^2(\theta) + \frac{\omega_{\mathrm{M}}P(1-P)\sin^2(\theta)}{\omega_0 + \omega_{\mathrm{M}}\lambda_{\mathrm{ex}}k^2}\,. \tag{12.36}$$

The corresponding eigenstate has the same form and properties as the eigenstate of spin waves in bulk ferromagnets and is given by

$$\mathbf{m}(k) = \frac{N}{\sqrt{\omega_{\mathrm{fx}}\omega_{\mathrm{fy}}}}\begin{bmatrix} i\omega_{\mathrm{fy}} \\ \sqrt{\omega_{\mathrm{fx}}\omega_{\mathrm{fy}}} \end{bmatrix} \tag{12.37}$$

with N a dimensionless normalization constant.

In the limit of large wavevectors, i.e. the exchange limit $\lambda_{\mathrm{ex}}k^2 \gg 1$, the dispersion relation reduces to (12.27) that was derived for bulk magnetic media. However, in the dipolar limit of small k-values, $\lambda_{\mathrm{ex}}k^2 \ll 1$, the dispersion relation differs from that in bulk ferromagnetic media. Again, two limiting cases are found for $\theta = 0$ and $\theta = \pi/2$.

For $\lambda_{\mathrm{ex}}k^2 \ll 1$ and $\theta = 0$, the dispersion relation becomes

$$\omega_{\mathrm{BVW}}^2 = \omega_0\left(\omega_0 + \omega_{\mathrm{M}}\frac{1 - e^{-kd}}{kd}\right)\,. \tag{12.38}$$

The propagation direction of these waves is parallel to the direction of the static equilibrium magnetization. Their dispersion relation is plotted in Fig. 12.1 for a 30 nm thick Ni film with $M_{\mathrm{s}} = 480$ kA/m [32], $A_{\mathrm{ex}} = 8$ pJ/m [33], and an external magnetic field of $\mu_0 H_{\mathrm{ext}} = 50$ mT. According to the dispersion relation, the frequency decreases with increasing wavenumber, and thus the group velocity, which is defined as $\mathbf{v}_{\mathrm{g}} = \partial\omega/\partial\mathbf{k}$, is negative. On the other hand, the phase velocity $\mathbf{v}_{\mathrm{p}} = \mathbf{k}\,\omega/k^2$, which describes the velocity and direction of the phase front, is positive. The energy flow of a wave is always parallel to the group velocity, and thus in this geometry, the energy flow and the group velocity are antiparallel to the wavevector and the phase velocity. For this reason, such waves are called backward volume waves (BVWs). As shown in Fig. 12.1, when the exchange interaction becomes non-negligible at larger wavevectors, the dispersion relation shifts to higher frequencies. This effect increases for higher k-values, finally reaching the limiting case of exchange-dominated spin waves.

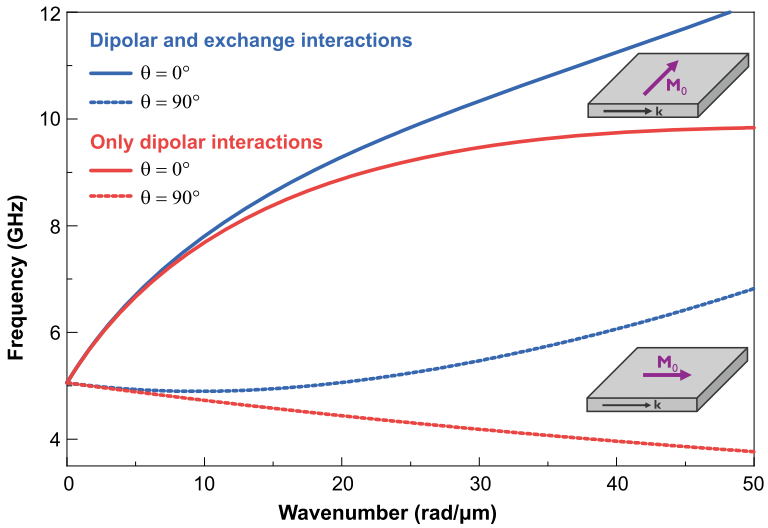

Fig. 12.1 Spin wave dispersion according to (12.35) for a 30 nm thick Ni film. Material parameters are $M_s = 480\,\text{kA/m}$ and $A_{ex} = 8\,\text{pJ/m}$, whereas the external magnetic field is $\mu_0 H_{ext} = 50\,\text{mT}$. The solid red and blue lines correspond to dispersion relations of dipolar and dipolar–exchange surface spin waves, respectively. The dashed red and blue lines correspond to dispersion relations of dipolar and dipolar–exchange backward volume spin waves, respectively

In the dipolar limit ($\lambda_{ex} k^2 \ll 1$), the dispersion relation for $\theta = \pi/2$ becomes

$$\omega_{SW}^2 = \omega_0(\omega_0 + \omega_M) + \omega_M^2 \left(1 - \frac{1 - e^{-kd}}{kd}\right) \frac{1 - e^{-kd}}{kd}. \tag{12.39}$$

These waves are called surface waves since their amplitude decays exponentially away from the surface. However, if the film is sufficiently thin, the magnetization can be considered uniform over the film thickness as mentioned earlier. The dispersion relations of spin waves both in the dipolar approximation and when the dipolar and exchange interaction are simultaneously present are plotted in Fig. 12.1. The group velocity of these waves is positive and thus points in the same direction as the phase velocity.

It should also be mentioned that spin waves are accompanied by a dynamic electric field. This electric field $\mathbf{e}$ is obtained from Maxwell's equations (12.3) and (12.5) which can be rewritten as

$$\nabla \cdot \mathbf{e} = 0 \tag{12.40}$$

$$\nabla \times \mathbf{e} = -i\mu_0\omega(\mathbf{h}_{dip} + \mathbf{m}) = -i\mu_0\omega\left(\bar{N}_{dip} + \bar{I}\right)\mathbf{m} \tag{12.41}$$

with $\bar{I}$ the identity matrix. Equation (12.41) indicates that both the dynamic dipolar field and the dynamic magnetization contribute to the generation of the dynamic

electric field. However, in the magnetostatic limit when $k_0 \ll k$, the effect of the dipolar field is much smaller than that of the dynamic magnetization. Taking this into account and solving Maxwell's equations for plane waves results in

$$\mathbf{e} = -\frac{\mu_0 \omega}{k^2} \mathbf{k} \times \mathbf{m} \tag{12.42}$$

for the dynamic electric field [20].

For spin waves at GHz frequencies in ferromagnetic media, the energy stored in the electric field is much smaller than the energy stored in the magnetic system [20]. Therefore, the magnetostatic waves can be considered as "magnetization waves". Note that this applies to spin waves in both the dipolar and exchange regime. In both cases, at GHz frequencies, the wavelength of a spin wave is much shorter than the wavelength of an electromagnetic wave in vacuum and the magnetostatic approximation is thus valid.

All calculations in this section are only valid at GHz frequencies in the magnetostatic limit. At higher frequencies near the THz regime, the spin wave wavelength becomes comparable to the wavelength of the electromagnetic wave in vacuum, $k_{\mathrm{sw}} \approx k_0$, and the magnetostatic approximation does not longer hold. At these higher frequencies, the influence of the time-varying electric field alters the wave behavior. This can be seen by considering both generation mechanisms of the magnetic field. As mentioned earlier, the dipolar magnetic field can be generated by both varying electric fields over time and by varying magnetization over space. The generation mechanism via the time varying electric field is proportional to the regular electromagnetic wave wavenumber k_0, whereas the generation mechanism via the magnetization is proportional to the magnetization wavenumber k_{sw}. Hence, the mechanism which governs the highest wavenumber dominates the generation of the magnetic dipolar field.

In the GHz regime and magnetostatic limit $k_0 \ll k_{\mathrm{sw}}$, the dipolar field generation is thus dominated by the variation of the magnetization over space. However, at much higher frequencies near the THz regime, both wavenumbers are of the same order and thus both generation mechanisms are of similar magnitude. This means that the generation of the magnetic dipolar field by the time varying electric field cannot be neglected anymore.

The frequency, for which the magnetostatic approximation breaks down, ω_{crit}, can be found by relating the wavenumbers to the frequency via the dispersion relations. The crossing point of the spin-wave dispersion relation, (12.27), with the linear electromagnetic dispersion relation, $\omega_0 = ck_0$, determines ω_{crit} and is given by

$$\omega_{\mathrm{crit}} = \frac{c^2}{\omega_{\mathrm{M}} \lambda_{\mathrm{ex}}} \tag{12.43}$$

with c the speed of light in vacuum. For frequencies $\omega \ll \omega_{\mathrm{crit}}$, the magnetostatic limit is valid and regular spin waves are obtained. For frequencies above ω_{crit}, spin waves behave similarly to classical electromagnetic waves with a considerable frac-

tion of energy stored in the dynamic electric field. As a result, besides the dipolar and exchange regime, there also exist a regular electromagnetic regime at higher frequencies, which corresponds to electromagnetic waves with a linear dispersion relation.

12.3 Elastic Waves

In the previous section, the properties of spin waves in ferromagnetic media, both in bulk materials and in thin films, have been discussed. In this section, we turn to the properties of wave-like oscillations of the displacement, i.e. elastic waves. We start with a short derivation of the fundamental equations of linear elasticity. Then, the different types of elastic waves and their characteristics are described.

12.3.1 Elastodynamic Equations of Motion

The equation of motion for the displacement $\mathbf{u}$ is given by

$$\rho \frac{d^2\mathbf{u}}{dt^2} = \nabla \cdot \bar{\sigma} + \mathbf{f}_\mathrm{b} \tag{12.44}$$

with ρ the mass density (kgm^{-3}), $\bar{\sigma}$ the two dimensional stress tensor with components σ_ij (Nm^{-2}), and $\mathbf{f}_\mathrm{b}$ the body forces acting on the material (Nm^{-3}). For linear elastic materials, the stress tensor is related to the strain tensor via Hooke's law

$$\bar{\sigma} = \bar{\bar{C}} : \bar{\varepsilon} \qquad \text{or} \qquad \sigma_\mathrm{ij} = \sum_{k=1}^{3}\sum_{l=1}^{3} C_\mathrm{ijkl}\varepsilon_\mathrm{kl}\,. \tag{12.45}$$

Here, $\bar{\bar{C}}$ is the fourth-order stiffness tensor and $\bar{\varepsilon}$ is the second-order strain tensor. The symmetries of the stiffness tensor allows to rewrite Hooke's law in reduced dimensionality [34, 35] as

$$\begin{bmatrix}\sigma_{11}\\ \sigma_{22}\\ \sigma_{33}\\ \sigma_{12}\\ \sigma_{13}\\ \sigma_{23}\end{bmatrix} = \begin{bmatrix} C_{11} & C_{12} & C_{13} & C_{14} & C_{15} & C_{16}\\ & C_{22} & C_{23} & C_{24} & C_{25} & C_{26}\\ & & C_{33} & C_{34} & C_{35} & C_{36}\\ & & & C_{44} & C_{45} & C_{46}\\ & \text{symm.} & & & C_{55} & C_{56}\\ & & & & & C_{66}\end{bmatrix} \begin{bmatrix}\varepsilon_{11}\\ \varepsilon_{22}\\ \varepsilon_{33}\\ 2\varepsilon_{12}\\ 2\varepsilon_{13}\\ 2\varepsilon_{23}\end{bmatrix}. \tag{12.46}$$

This is called the Voigt notation for Hooke's law. Important to note is the notation for the shear strain elements. In some works, this is given by the engineering strains $\gamma_{ij} = 2\varepsilon_{ij}$ which gives a factor of 2 difference with the real shear strains.

Equation (12.46) indicates that a material with a nonsymmetric (e.g. triclinic) crystal structure is described by 21 independent stiffness coefficients [36, 37]. In a crystal system with a certain symmetry, the number of independent stiffness constants can be greatly reduced. For example, only three independent stiffness constants are required to describe cubic crystal systems. The stiffness tensor then becomes

$$\bar{C}_{\text{cubic}} = \begin{bmatrix} C_{11} & C_{12} & C_{12} & 0 & 0 & 0 \\ & C_{11} & C_{12} & 0 & 0 & 0 \\ & & C_{11} & 0 & 0 & 0 \\ & & & C_{44} & 0 & 0 \\ & \text{symm.} & & & C_{44} & 0 \\ & & & & & C_{44} \end{bmatrix}. \tag{12.47}$$

In this case, the residual anisotropy can be quantified by the Zener factor A, which is given by

$$A = \frac{2C_{44}}{C_{11} - C_{12}}. \tag{12.48}$$

A Zener factor of 1 indicates fully isotropic elastic properties. In this isotropic limit, only two independent constants are necessary to describe the stiffness tensor. Note that different combinations of parameters can be used to represent the isotropic case, such as Young's modulus and the Poisson ratio, Young's modulus and the shear modulus, or the Lamé moduli. All descriptions are fully equivalent [37, 38].

For small displacements, the relation between the strain and displacement is given by [34, 36]

$$\bar{\varepsilon} = \frac{1}{2}\left(\nabla\mathbf{u} + (\nabla\mathbf{u})^T - \nabla\mathbf{u}\,(\nabla\mathbf{u})^T\right) \approx \frac{1}{2}\left(\nabla\mathbf{u} + (\nabla\mathbf{u})^T\right). \tag{12.49}$$

Combining (12.44), (12.47), and (12.49) results in the elastodynamic equations of motion with the displacement as the only variable. For a material with cubic symmetry, the equations are given by

$$\begin{aligned}
\rho\frac{\partial^2 u_x}{\partial t^2} &= C_{11}\frac{\partial^2 u_x}{\partial x^2} + C_{44}\left(\frac{\partial^2 u_x}{\partial y^2} + \frac{\partial^2 u_x}{\partial z^2}\right) + (C_{12} + C_{44})\left(\frac{\partial^2 u_y}{\partial x \partial y} + \frac{\partial^2 u_z}{\partial x \partial z}\right) + f_x \\
\rho\frac{\partial^2 u_y}{\partial t^2} &= C_{11}\frac{\partial^2 u_y}{\partial y^2} + C_{44}\left(\frac{\partial^2 u_y}{\partial x^2} + \frac{\partial^2 u_y}{\partial z^2}\right) + (C_{12} + C_{44})\left(\frac{\partial^2 u_x}{\partial x \partial y} + \frac{\partial^2 u_z}{\partial y \partial z}\right) + f_y \\
\rho\frac{\partial^2 u_z}{\partial t^2} &= C_{11}\frac{\partial^2 u_z}{\partial z^2} + C_{44}\left(\frac{\partial^2 u_z}{\partial x^2} + \frac{\partial^2 u_z}{\partial y^2}\right) + (C_{12} + C_{44})\left(\frac{\partial^2 u_x}{\partial x \partial z} + \frac{\partial^2 u_y}{\partial y \partial z}\right) + f_z.
\end{aligned} \tag{12.50}$$

Note that the above equations do not contain any damping terms and the system is assumed to be lossless. In practice, materials always possess some degree of viscoelasticity. In this case, the energy in the elastic wave is lost by different mechanisms such as phonon–phonon scattering due to the anharmonicity of the vibrational potential or the scattering of phonons by impurities. This can be taken into account by considering complex stiffness coefficients [37, 38]. However, in the following, perfect elasticity without loss is assumed for simplicity.

12.3.2 Elastic Waves in Thin Films

In this section, we introduce the properties of elastic waves in an idealized thin film with free surfaces. This corresponds to an isolated thin film in vacuum in which the elastodynamics is perfectly confined inside the film. The perfect confinement is achieved by large acoustical impedance mismatch between the film and vacuum. Therefore, the model also approximately represents a thin film surrounded by materials with strongly different acoustic impedances, e.g. a film with a free top surface and a large acoustic impedance mismatch with the supporting substrate. For more realistic approaches, appropriate stress and velocity boundary conditions need to be applied at the interfaces. In the next section, when the magnetoelastic interaction is included, it is demonstrated that the magnetization dynamics also generate elastic stresses, which further complicates the description at the boundaries. In such cases, an analytical treatment of the system is difficult and accurate studies require numerical simulations, e.g. by finite element methods. Nonetheless, the treatment of an idealized system presented here provides analytical insights in the basic elastic (and magnetoelastic) behavior. This insight will help in the understanding of the magnetoelastic waves in the next section and can be used in the future to interpret numerical simulations of more realistic systems.

For the case of thin films with free surface boundary conditions, the variation of the displacement along the thickness of the film is much smaller than the in-plane variation. Hence, the derivative of the displacement along the film surface normal can be neglected with respect to the derivatives in the in-plane directions, i.e. $\partial u/\partial y \ll \partial u/\partial x\,,\, \partial u/\partial z$. The elastodynamic equations of motion for a thin film with a surface normal in the y-direction are then given by

$$\begin{aligned}
\rho\frac{\partial^2 u_\mathrm{x}}{\partial t^2} &= C_{11}\frac{\partial^2 u_\mathrm{x}}{\partial x^2} + C_{44}\frac{\partial^2 u_\mathrm{x}}{\partial z^2} + (C_{12}+C_{44})\frac{\partial^2 u_\mathrm{z}}{\partial x\partial z}\\
\rho\frac{\partial^2 u_\mathrm{y}}{\partial t^2} &= C_{44}\left(\frac{\partial^2 u_\mathrm{y}}{\partial x^2} + \frac{\partial^2 u_\mathrm{y}}{\partial z^2}\right)\\
\rho\frac{\partial^2 u_\mathrm{z}}{\partial t^2} &= C_{11}\frac{\partial^2 u_\mathrm{z}}{\partial z^2} + C_{44}\frac{\partial^2 u_\mathrm{z}}{\partial x^2} + (C_{12}+C_{44})\frac{\partial^2 u_\mathrm{x}}{\partial x\partial z}\,.
\end{aligned} \tag{12.51}$$

The above set of linear differential equations has wave-like solutions of the form [15, 37]

$$\mathbf{u}(\mathbf{r}, t) = \begin{bmatrix} u_\mathrm{x} \\ u_\mathrm{y} \\ u_\mathrm{z} \end{bmatrix} e^{i(\omega t + \mathbf{k}\cdot\mathbf{r})} . \tag{12.52}$$

To determine the dispersion relation of elastic waves in thin films, (12.52) is substituted into the wave equations (12.51). Rewriting the system in matrix notation and considering that the wavevector $\mathbf{k}$ points along the x-direction, results in

$$\begin{bmatrix} \omega^2 - v_l^2 k^2 & 0 & 0 \\ 0 & \omega^2 - v_\mathrm{t}^2 k^2 & 0 \\ 0 & 0 & \omega^2 - v_\mathrm{t}^2 k^2 \end{bmatrix} \begin{bmatrix} u_\mathrm{x} \\ u_\mathrm{y} \\ u_\mathrm{z} \end{bmatrix} = 0 \tag{12.53}$$

with $v_l = \sqrt{C_{11}/\rho}$ the velocity of the longitudinal wave, $v_\mathrm{t} = \sqrt{C_{44}/\rho}$ the velocity of the transversal wave, and ω the angular frequency of the elastic wave. As a result, three independent elastic waves are found, which correspond to the three components of the displacement vector.

When only the u_x component is nonzero, longitudinal waves are formed since the displacement oscillation is in the same direction as the wavevector. This wave is also called a compressional or dilational wave. The dispersion relation, $\omega_l(k)$, of this wave is easily found from (12.53) to be $\omega_l = v_l k$ [15, 36, 37]. The dispersion relation is linear, and thus the group velocity v_l equals the phase velocity, independently of frequency.

Waves with nonzero displacement components u_y and u_z oscillate perpendicular to the propagation direction. Therefore, these waves are transversal waves, also called shear or rotational waves. Their dispersion relation is also linear and equals $\omega_\mathrm{t} = v_\mathrm{t} k$ [15, 36, 37]. The phase and group velocities are thus both equal to v_t. It is further possible to classify these waves based on their polarization with respect to the film surface. The u_y component corresponds to shear vertical (SV) waves and the u_z component corresponds to shear horizontal (SH) waves. It is important to note that the velocity of the longitudinal wave is always larger than the velocity of the shear waves because $C_{11} > C_{44}$ [36, 37].

The energy of elastic waves oscillates between the elastic potential energy and the kinetic energy. The elastic energy density is given by [15, 36, 37]

$$\mathcal{E}_\mathrm{el} = \frac{1}{2}\bar{\sigma} : \bar{\varepsilon} = \frac{1}{2} C_{ijkl}\varepsilon_{ij}\varepsilon_{kl} = \frac{1}{2}\sum_{i=1}^{3}\sum_{j=1}^{3}\sum_{k=1}^{3}\sum_{l=1}^{3} C_{ijkl}\varepsilon_{ij}\varepsilon_{kl} \tag{12.54}$$

or in Voigt notation

$$\mathcal{E}_\mathrm{el} = \frac{1}{2}\bar{\sigma} : \bar{\varepsilon} = \frac{1}{2} C_{ij}\varepsilon_j\varepsilon_i , \tag{12.55}$$

whereas the kinetic energy density is given by

$$\mathcal{E}_{\text{kin}} = \frac{\rho ||\mathbf{v}||^2}{2} \qquad \text{with} \qquad \mathbf{v} = \frac{\partial \mathbf{u}}{\partial t} \,. \tag{12.56}$$

Hence, for an elastic wave, the total energy is $\mathcal{E}_{\text{tot}} = \mathcal{E}_{\text{el}} + \mathcal{E}_{\text{kin}}$ and $\mathcal{E}_{\text{el}} = \mathcal{E}_{\text{kin}}$.

12.4 Magnetoelastic Waves

In the two previous sections, magnetic and elastic waves in thin films were studied. This section connects the two previous sections by introducing magnetoelastic interactions. In the first part of this section, the magnetoelastic interaction terms are described, which couple magnetic and elastic waves. In the second part, the properties of these magnetoelastic waves are derived and explained. Magnetoelastic waves have been studied in detail in bulk materials [8–10], at free surfaces [39–41], and in infinitesimally thin films [11, 12]. This section reviews the most important aspects of these magnetoelastic waves together with the corresponding equations. Beyond this review, we subsequently derive the influence of finite film thickness on the properties of the magnetoelastic waves by taking into account the appropriate dipolar and exchange fields.

12.4.1 Magnetoelastic Interactions

Magnetoelastic interactions can be separated in two different effects: firstly, the influence of the direction of the magnetization on the internal strain in a ferromagnet, called the magnetostrictive effect; and secondly, the effect of strain on the magnetization state, called the Villari effect. If both effects are considered simultaneously, one speaks about magnetoelasticity.

12.4.1.1 Magnetostriction

Magnetostriction describes how the magnetization affects the elastic behavior of a material. Therefore, in a magnetostrictive material, different magnetization states result in different strain states. For a material with cubic symmetry, the magnetoelastic energy density is given by [8]

$$\begin{aligned}\mathcal{E}_{\text{mel}} = &\frac{B_1}{M_\text{s}^2}\left(\varepsilon_{\text{xx}}\left(M_\text{x}^2 - \frac{1}{3}\right) + \varepsilon_{\text{yy}}\left(M_\text{y}^2 - \frac{1}{3}\right) + \varepsilon_{\text{zz}}\left(M_\text{z}^2 - \frac{1}{3}\right)\right) \\ &+ \frac{2B_2}{M_\text{s}^2}\left(\varepsilon_{\text{xy}} M_\text{x} M_\text{y} + \varepsilon_{\text{yz}} M_\text{y} M_\text{z} + \varepsilon_{\text{zx}} M_\text{x} M_\text{z}\right)\end{aligned} \tag{12.57}$$

with B_1 and B_2 the linear isotropic and anisotropic magnetoelastic coupling constants, respectively (Jm^{-3}). It is worth noting that the magnitude of the saturation magnetization has no influence on the magnetoelastic energy or strain state, which are rather determined by the orientation of the magnetization vector. The magnetization orientation is defined by the vector

$$\boldsymbol{\zeta} = \begin{bmatrix} \zeta_\mathrm{x} \\ \zeta_\mathrm{y} \\ \zeta_\mathrm{z} \end{bmatrix} = \frac{1}{M_\mathrm{s}} \begin{bmatrix} M_\mathrm{x} \\ M_\mathrm{y} \\ M_\mathrm{z} \end{bmatrix} . \tag{12.58}$$

Substituting this into (12.57) leads to

$$\begin{aligned} \mathcal{E}_\mathrm{mel} =& B_1 \left(\varepsilon_\mathrm{xx} \left(\zeta_\mathrm{x}^2 - \frac{1}{3} \right) + \varepsilon_\mathrm{yy} \left(\zeta_\mathrm{y}^2 - \frac{1}{3} \right) + \varepsilon_\mathrm{zz} \left(\zeta_\mathrm{z}^2 - \frac{1}{3} \right) \right) \\ &+ 2B_2 \left(\varepsilon_\mathrm{xy} \zeta_\mathrm{x} \zeta_\mathrm{y} + \varepsilon_\mathrm{yz} \zeta_\mathrm{y} \zeta_\mathrm{z} + \varepsilon_\mathrm{zx} \zeta_\mathrm{x} \zeta_\mathrm{z} \right) . \end{aligned} \tag{12.59}$$

Based on this expression for the magnetoelastic energy density, it is possible to calculate the magnetostrictive body force, which is given by

$$\mathbf{f}_\mathrm{mel} = \nabla \cdot \bar{\sigma}_\mathrm{mel} = \nabla \cdot \left(\frac{d\mathcal{E}_\mathrm{mel}}{d\varepsilon_\mathrm{ij}} \right) , \tag{12.60}$$

leading to

$$\mathbf{f}_\mathrm{mel} = 2B_1 \begin{bmatrix} \zeta_\mathrm{x} \frac{\partial \zeta_\mathrm{x}}{\partial \mathrm{x}} \\ \zeta_\mathrm{y} \frac{\partial \zeta_\mathrm{y}}{\partial y} \\ \zeta_\mathrm{z} \frac{\partial \zeta_\mathrm{z}}{\partial z} \end{bmatrix} + B_2 \begin{bmatrix} \zeta_\mathrm{x} \left(\frac{\partial \zeta_\mathrm{y}}{\partial y} + \frac{\partial \zeta_\mathrm{z}}{\partial z} \right) + \zeta_\mathrm{y} \frac{\partial \zeta_\mathrm{x}}{\partial y} + \zeta_\mathrm{z} \frac{\partial \zeta_\mathrm{x}}{\partial z} \\ \zeta_\mathrm{y} \left(\frac{\partial \zeta_\mathrm{x}}{\partial x} + \frac{\partial \zeta_\mathrm{z}}{\partial z} \right) + \zeta_\mathrm{x} \frac{\partial \zeta_\mathrm{y}}{\partial x} + \zeta_\mathrm{z} \frac{\partial \zeta_\mathrm{y}}{\partial z} \\ \zeta_\mathrm{z} \left(\frac{\partial \zeta_\mathrm{x}}{\partial x} + \frac{\partial \zeta_\mathrm{y}}{\partial y} \right) + \zeta_\mathrm{x} \frac{\partial \zeta_\mathrm{z}}{\partial x} + \zeta_\mathrm{y} \frac{\partial \zeta_\mathrm{z}}{\partial y} \end{bmatrix} . \tag{12.61}$$

There are three important parameters that determine the strength of the magnetostrictive body force: the magnetoelastic coupling constants, the magnetization orientation, and the gradient of the magnetization orientation.

The magnetostrictive body force affects the elastodynamics and thus needs to be added to the elastodynamic equation (12.44) in magnetostrictive media. This allows for the analytical description of the influence of the magnetization direction on the elastodynamics and the properties of (magneto-)elastic waves.

Another important quantity is the magnetostrictive strain, which is the additional strain originating from the magnetostrictive effect. For a material with cubic symmetry, the magnetostrictive strain is given by [24, 42, 43]

$$\bar{\varepsilon}_\mathrm{mel} = \frac{3}{2} \begin{bmatrix} \lambda_{100} \left(\zeta_\mathrm{x}^2 - \frac{1}{3} \right) & \lambda_{111} \zeta_\mathrm{x} \zeta_\mathrm{y} & \lambda_{111} \zeta_\mathrm{x} \zeta_\mathrm{z} \\ \lambda_{111} \zeta_\mathrm{y} \zeta_\mathrm{x} & \lambda_{100} \left(\zeta_\mathrm{y}^2 - \frac{1}{3} \right) & \lambda_{111} \zeta_\mathrm{y} \zeta_\mathrm{z} \\ \lambda_{111} \zeta_\mathrm{z} \zeta_\mathrm{x} & \lambda_{111} \zeta_\mathrm{z} \zeta_\mathrm{y} & \lambda_{100} \left(\zeta_\mathrm{z}^2 - \frac{1}{3} \right) \end{bmatrix} . \tag{12.62}$$

with λ_{100} and λ_{111} the magnetostriction coefficients representing the maximum magnetostrictive strain for fully-saturated magnetization along the $\langle 100 \rangle$ or $\langle 111 \rangle$ crystallographic directions, respectively.

The magnetostriction coefficients are related to the magnetoelastic coupling constants by

$$\lambda_{100} = \frac{2}{3} \frac{B_1}{C_{12} - C_{11}}, \qquad \lambda_{111} = -\frac{B_2}{3C_{44}}. \tag{12.63}$$

Hence, it is also possible to express the magnetostrictive body force as a function of the magnetostrictive strain via

$$\mathbf{f}_{\text{mel}} = \nabla \cdot \bar{\sigma}_{\text{mel}} = \nabla \cdot \left(\bar{\bar{C}} : \bar{\varepsilon}_{\text{mel}} \right). \tag{12.64}$$

Note that for an isotropic material, $\lambda_{100} = \lambda_{111} = \lambda_{\text{eq}}$ and $B_1 = B_2 = B$.

12.4.1.2 The Villari Effect

The Villari effect describes how elastic strain affects the magnetization state and is also called the inverse magnetostrictive effect. Strain in a magnetostrictive material results in an effective magnetoelastic field, which can be derived from (12.2) and (12.57). For a material with cubic symmetry, the magnetoelastic effective field is

$$\mathbf{H}_{\text{mel}} = -\frac{1}{\mu_0} \frac{d\mathcal{E}_{\text{mel}}}{d\mathbf{M}} = -\frac{2}{\mu_0 M_{\text{s}}} \begin{bmatrix} B_1 \varepsilon_{\text{xx}} \zeta_{\text{x}} + B_2 (\varepsilon_{\text{xy}} \zeta_{\text{y}} + \varepsilon_{zx} \zeta_{\text{z}}) \\ B_1 \varepsilon_{\text{yy}} \zeta_{\text{y}} + B_2 (\varepsilon_{\text{xy}} \zeta_{\text{x}} + \varepsilon_{yz} \zeta_{\text{z}}) \\ B_1 \varepsilon_{\text{zz}} \zeta_{\text{z}} + B_2 (\varepsilon_{\text{zx}} \zeta_{\text{x}} + \varepsilon_{yz} \zeta_{\text{y}}) \end{bmatrix} \tag{12.65}$$

with ζ_i the normalized magnetization components, as defined by (12.58). The resulting magnetization dynamics are described by the LLG equation (12.1), including the above magnetoelastic field as a contribution to $\mathbf{H}_{\text{eff}}$.

12.4.2 Magnetoelastic Waves in Thin Films

When the magnetoelastic interaction terms $\mathbf{f}_{\text{mel}}$ and $\mathbf{H}_{\text{mel}}$ are combined with the magnetodynamic equation (12.1) and the elastodynamic equation (12.51), a set of coupled differential equations is obtained. Formally, these differential equations are nonlinear because the terms originating from the magnetoelastic interaction show a quadratic dependence on the magnetization and the displacement. Therefore, the magnetoelastic effect formally results in a nonlinear interaction. However, when the dynamic components are assumed to be weak, the differential equations can be linearized. In this case, wave-like solutions for the magnetization and the displacement,

given by (12.14) and (12.52), exist for the coupled set of equations. These solutions correspond to magnetoelastic waves. However, it is important to keep in mind that for large dynamic components, a system of nonlinear differential equations has to be solved, including nonlinear magnetoelastic interaction effects.

To reduce the complexity of the calculations, a homogeneous and isotropic material is assumed. The geometry of the structure remains the same as in the previous sections with the film in the xz-plane and the y-direction normal to the film surface. The static magnetization and the static external field are chosen along the z-direction, as in Sect. 12.2.3. Then, substituting the wave-like ansatz into the equations of motion and neglecting terms quadratic in $\mathbf{m}$ or $\mathbf{u}$, leads to the following linearized system of equations:

$$\begin{aligned}
-\rho\omega^2 u_\mathrm{x} &= -C_{11}k_\mathrm{x}^2 u_\mathrm{x} - C_{44}k_\mathrm{z}^2 u_\mathrm{x} - (C_{12}+C_{44})k_\mathrm{x}k_\mathrm{z}u_\mathrm{z} + \frac{B_2}{M_\mathrm{s}} i k_\mathrm{z} m_\mathrm{x} \\
-\rho\omega^2 u_\mathrm{y} &= -C_{44}\left(k_\mathrm{x}^2 u_\mathrm{y} + k_\mathrm{z}^2 u_\mathrm{y}\right) + \frac{B_2}{M_\mathrm{s}} i k_\mathrm{z} m_\mathrm{y} \\
-\rho\omega^2 u_\mathrm{z} &= -C_{11}k_\mathrm{z}^2 u_\mathrm{z} - C_{44}k_\mathrm{x}^2 u_\mathrm{z} - (C_{12}+C_{44})k_\mathrm{x}k_\mathrm{z}u_\mathrm{x} + \frac{B_2}{M_\mathrm{s}} i k_\mathrm{x} m_\mathrm{x} \\
i\omega m_\mathrm{x} &= -\omega_\mathrm{fy} m_\mathrm{y} - \gamma B_2 i k_\mathrm{z} u_\mathrm{y} \\
i\omega m_\mathrm{y} &= \omega_\mathrm{fx} m_\mathrm{x} + \gamma B_2 i \left(k_\mathrm{z} u_\mathrm{x} + k_\mathrm{x} u_\mathrm{z}\right) .
\end{aligned} \tag{12.66}$$

Assuming that the elastic properties of the thin film are isotropic, the C_{12} stiffness constant can be replaced by $C_{12} = C_{11} - 2C_{44}$. Moreover, as discussed above, two types of elastic waves exist in in an isotropic material, i.e. longitudinal and transversal waves. Therefore, it is convenient to define new displacement variables parallel (u_l) and perpendicular (u_t) to the propagation direction such that

$$u_\mathrm{x} = u_l \sin(\theta) + u_\mathrm{t} \cos(\theta) , \qquad u_\mathrm{z} = u_l \cos(\theta) - u_\mathrm{t} \sin(\theta) . \tag{12.67}$$

Here, θ is the angle between the static magnetization $\mathbf{M}_0$ and the propagation direction $\mathbf{k}$. Substituting these redefined displacement components into the dynamic equation of motion together with $k_\mathrm{x} = k\sin(\theta)$ and $k_\mathrm{z} = k\cos(\theta)$ results in

$$\begin{aligned}
(\omega^2 - \omega_l^2)\sin(\theta)u_l + (\omega^2 - \omega_\mathrm{H})\cos(\theta)u_\mathrm{t} + \frac{iBk\cos(\theta)}{\rho M_s} m_\mathrm{x} &= 0 \\
(\omega^2 - \omega_\mathrm{V}^2)u_\mathrm{y} + \frac{iBk\cos(\theta)}{\rho M_s} m_\mathrm{y} &= 0 \\
(\omega^2 - \omega_l^2)\cos(\theta)u_l - (\omega^2 - \omega_\mathrm{H}^2)\sin(\theta)u_\mathrm{t} + \frac{iBk\sin(\theta)}{\rho M_s} m_\mathrm{x} &= 0 \\
i\gamma Bk\cos(\theta)u_\mathrm{y} + i\omega m_\mathrm{x} + \omega_\mathrm{fy} m_\mathrm{y} &= 0 \\
i\gamma Bk\sin(2\theta)u_l + i\gamma Bk\cos(2\theta)u_\mathrm{t} + \omega_\mathrm{fx} m_\mathrm{x} - i\omega m_\mathrm{y} &= 0
\end{aligned} \tag{12.68}$$

with ω the angular frequency of the magnetoelastic wave, $\omega_l = v_l k = \sqrt{\frac{C_{11}}{\rho}} k$ the dispersion relation of longitudinal elastic waves, $\omega_\mathrm{H} = v_\mathrm{t} k = \sqrt{\frac{C_{44}}{\rho}} k$ the dispersion relation of horizontally-polarized (in-plane) transversal elastic waves, and $\omega_\mathrm{V} = \omega_\mathrm{H}$ the dispersion relation of vertically-polarized (out-of-plane) transversal elastic waves. Here, the distinction between ω_V and ω_H is made to keep track of the origin of different terms in the equations of motion.

Note that this set of equations describes magnetoelastic waves in thin films with finite thickness. The finite thickness of the film changes the dipolar field according to (12.30) and consequently also the properties of the magnetoelastic waves. The thickness influence is captured by the parameters ω_fx and ω_fy. In the following, different cases and geometries of magnetoelastic wave solutions of the coupled equations of motion are discussed.

12.4.2.1 Wave Propagation Perpendicular to the Magnetization

We first consider the case in which the wave propagation direction is perpendicular to the static equilibrium magnetization, i.e. $\theta = \pi/2$. In this geometry, (12.68) indicates that the magnetoelastic body force $\mathbf{f}_\mathrm{mel}$ only acts on the u_t component of the displacement. Conversely, only the displacement component u_t generates a magnetoelastic field that interacts with the magnetic system. Hence, only the in-plane transversal elastic wave couples to surface spin waves and vice versa. This means that the longitudinal and out-of-plane transversal elastic waves are independent of the magnetic system in a first-order approximation. As a consequence, their dispersion relations remain unchanged, i.e. $\omega_l = v_l k$ and $\omega_\mathrm{V} = v_t k$, respectively, as described in Sect. 12.3.

Eliminating all uncoupled equations and using $\theta = \pi/2$ in (12.68), the system becomes

$$\begin{bmatrix} \omega^2 - \omega_\mathrm{H}^2 & \frac{iBk}{\rho M_\mathrm{s}} & 0 \\ -i\gamma Bk & \omega_\mathrm{fx} & -i\omega \\ 0 & i\omega & \omega_\mathrm{fy} \end{bmatrix} \begin{bmatrix} u_\mathrm{t} \\ m_\mathrm{x} \\ m_\mathrm{y} \end{bmatrix} = 0 \tag{12.69}$$

with ω the angular frequency of the magnetoelastic wave and $\omega_\mathrm{H} = v_\mathrm{t} k$ the resonance frequency of the uncoupled horizontally-polarized transversal elastic wave. Note that in this geometry, the in-plane transversal displacement component is fully aligned in the z-direction, i.e. $u_\mathrm{t} = u_\mathrm{z}$. To obtain nontrivial solutions, the determinant of the linear system must vanish, which leads to the condition

$$(\omega^2 - \omega_\mathrm{H}^2)(\omega^2 - \omega_\mathrm{fm}^2) - Jk^2\omega_\mathrm{fy} = 0 \tag{12.70}$$

with

$$J = \frac{\gamma B^2}{\rho M_\mathrm{s}} \tag{12.71}$$

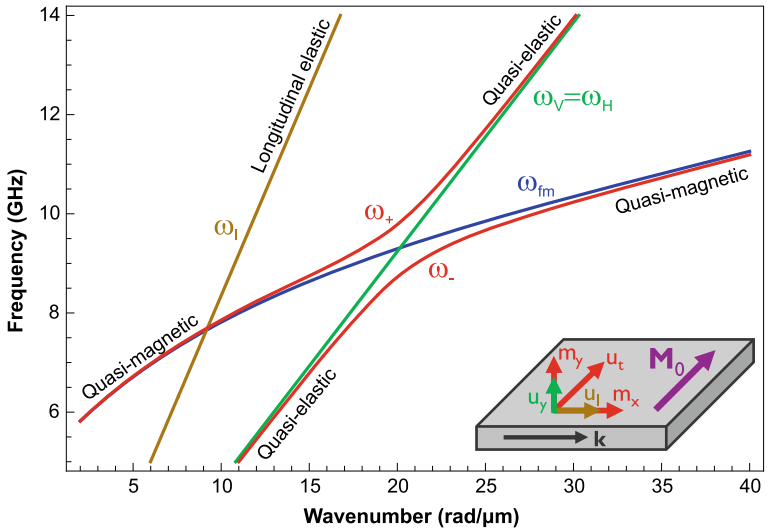

Fig. 12.2 Magnetoelastic wave dispersion relations according to (12.70) for a 30 nm thick Ni film and propagation direction perpendicular to the magnetization (red lines). The external magnetic field is $\mu_0 H_{\text{ext}} = 50\,\text{mT}$. For comparison, the dispersion relations of longitudinal and transversal elastic waves (brown and green lines, respectively) as well as uncoupled spin waves (blue line) are also shown

and $\omega_{\text{fm}} = \sqrt{\omega_{\text{fx}}\omega_{\text{fy}}}$ the uncoupled spin wave resonance frequency. Equation (12.70) has the general form of a dispersion relation of two interacting waves. Here, the first wave is a transversal elastic wave characterized by $\omega^2 - \omega_{\text{H}}^2 = 0$ and the second wave is a spin wave characterized by $\omega^2 - \omega_{\text{fm}}^2 = 0$. The interaction between these two waves is quantified by $Jk^2\omega_{\text{fy}}$. As expected, setting the magnetoelastic coupling constant B to zero leads to the original dispersion relations of uncoupled elastic and magnetic waves.

Equation (12.70) has two physically-meaningful solutions for ω, which are given by

$$\omega_{\pm}^2 = \frac{\omega_{\text{H}}^2 + \omega_{\text{fm}}^2}{2} \pm \sqrt{\left(\frac{\omega_{\text{fm}}^2 - \omega_{\text{H}}^2}{2}\right)^2 + Jk^2\omega_{\text{fy}}}\,. \tag{12.72}$$

These two solutions represent the dispersion relations of the resulting magnetoelastic waves. These dispersion relations together with the dispersion relations of the uncoupled elastic waves are plotted in Fig. 12.2 for a 30 nm thick Ni film. The magnetic parameters are the same as used in Fig. 12.1. The magnetoelastic coupling constant is $B = 10\,\text{MJ/m}^3$ [44, 45], the stiffness constants are $C_{11} = 245\,\text{GPa}$ and $C_{44} = 75\,\text{GPa}$ [46], and the mass density is $\rho = 8900\,\text{kg/m}^3$ [47]. The two linear dispersion relations correspond to the uncoupled elastic waves whereas the two red curves represent the dispersion relations of the magnetoelastic waves.

Figure 12.2 clearly shows that the two branches of the magnetoelastic wave dispersion relations do not cross each other. If the transversal elastic waves and the spin waves were not interacting, their dispersion relations would intersect. However, due to the magnetoelastic interaction, this crossing is avoided, leading to a gap between the two curves. This so-called anticrossing behavior of the dispersion relations is a typical characteristic of interacting waves [15, 16].

The gap formation is also visible in the equation of the dispersion relations, i.e. (12.72). At the point in reciprocal space where the dispersion relations of the uncoupled waves would intersect, i.e. $(\omega_{\text{cross}}, k_{\text{cross}})$, the term $\omega_{\text{fm}}^2 - \omega_{\text{H}}^2$ vanishes. At this condition, the interaction coefficient $Jk^2\omega_{\text{fy}}$ has a strong influence on the dispersion relation. When $Jk^2\omega_{\text{fy}} \gtrsim \omega_{\text{fm}}^2 - \omega_{\text{H}}^2$, the interaction between the magnetic and elastic system is strong, leading to the formation of coupled magnetoelastic waves. As a result, the anticrossing is formed, with a frequency gap that quantifies the strength of the interaction. This frequency gap is, to first order, given by

$$\Delta\omega(k_{\text{cross}}) \approx \frac{\sqrt{Jk_{\text{cross}}^2\omega_{\text{fy}}}}{\omega_{\text{cross}}} = \sqrt{\frac{\gamma B^2\omega_{\text{fy}}}{C_{44}M_0}} \tag{12.73}$$

where the relation $\omega_{\text{cross}} = \sqrt{\frac{C_{44}}{\rho}}k_{\text{cross}}$ was used. Note that ω_{fy} also depends on k_{cross} and that this approximation is only valid when $\Delta\omega(k_{\text{cross}}) < \omega_{\text{cross}}$. On the other hand, when $Jk^2\omega_{\text{fy}} \ll \omega_{\text{fm}}^2 - \omega_{\text{H}}^2$, the interaction term can be neglected, leading to nearly uncoupled elastic and magnetic waves. In this regime, the waves are called quasi-elastic or quasi-magnetic [15, 16]. Hence, the interaction between the elastic and magnetic waves is strongest when they are (nearly) degenerate, resulting in coupled magnetoelastic waves. By contrast, quasi-noninteracting waves are obtained when their frequencies and/or their wavelengths differ strongly.

The wavenumber at the crossing, k_{cross}, can be found by equalizing the dispersion relations of the noninteracting systems, i.e. $\omega_{\text{H}}(k_{\text{cross}}) = \omega_{\text{fm}}(k_{\text{cross}})$, and solving for k_{cross}. For the geometry considered here, the noninteracting dispersion relations are equal when

$$v_{\text{t}}k_{\text{cross}} = (\omega_0 + \omega_{\text{M}}\lambda_{\text{ex}}k_{\text{cross}}^2)^2 + \omega_{\text{M}}\left(\omega_0 + \omega_{\text{M}}\lambda_{\text{ex}}k_{\text{cross}}^2 + \omega_{\text{M}}(1-P)P\right), \tag{12.74}$$

which needs to be solved iteratively. Note that P is also a function of k_{cross} according to (12.30). Once k_{cross} is determined, the interaction coefficient $Jk^2\omega_{\text{fy}}$ and the gap amplitude can be calculated. In general, the coupling increases strongly for higher wavenumbers k_{cross}. This originates from the behavior of the magnetostriction and the Villari effect: a shorter wavelength leads to larger gradients of both displacement and magnetization. As a result, the magnetoelastic body force in (12.60) and the magnetoelastic field in (12.65) increase, leading to stronger interactions for higher k_{cross} values. This behavior opens possibilities to control the interaction strength by external parameters. For example, increasing an external magnetic field shifts the

spin wave dispersion relation to higher frequencies, leading to a larger value of k_{cross} and thus a stronger magnetoelastic coupling.

According to the dispersion relation in (12.72), two different wave-like solutions exist that correspond to two different magnetoelastic waves. To describe the characteristics of these waves, the corresponding eigenstates need to be calculated. They are given by

$$\begin{bmatrix} u_{\text{t}} \\ m_{\text{x}} \\ m_{\text{y}} \end{bmatrix} = N \begin{bmatrix} 1 \\ i\frac{\rho M_{\text{s}}}{Bk}(\omega_{\pm}^2 - \omega_{\text{H}}^2) \\ \frac{\rho M_{\text{s}}\omega_{\pm}}{Bk\omega_{\text{fy}}}(\omega_{\pm}^2 - \omega_{\text{H}}^2) \end{bmatrix} = N \begin{bmatrix} 1 \\ i\frac{\gamma Bk\omega_{\text{fy}}}{\omega_{\pm}^2 - \omega_{\text{fm}}^2} \\ \frac{\gamma Bk\omega_{\pm}}{\omega_{\pm}^2 - \omega_{\text{fm}}^2} \end{bmatrix} \tag{12.75}$$

with N a dimensionless normalization factor. Note that the polarization of the two magnetization components, for both cases ω_+ and ω_-, is clockwise (right-hand) elliptically polarized with ellipticity $\epsilon = |m_{\text{x}}|/|m_{\text{y}}| = \omega_{\text{fy}}/\omega_{\pm}$. The precession described by the u_{t} displacement and the m_{x} magnetization components is clockwise or counterclockwise (right-hand or left-hand) polarized, depending on the eigenstate ω_+ or ω_-.

Based on the eigenstate, it is possible to determine the variation of the energy associated with the different wave components during propagation. There is always a phase difference of $\pi/2$ between m_{x} and m_{y} as well as m_{x} and u_{t}. This indicates that, during propagation, the energy in the m_{x} component is transferred partially to the m_{y} and partially to the u_{t} component. Hence, for magnetoelastic waves, there is resonant energy transfer between the elastic and magnetic domains.

The three different regimes described by the dispersion relation in (12.72), i.e. the quasi-elastic, quasi-magnetic, and magnetoelastic regimes, are also seen from the eigenstates. In the quasi-elastic regime, the dispersion relation approaches the linear dispersion of the elastic waves, i.e. $\omega_{\pm}^2 - \omega_{\text{H}}^2 \approx 0$ and thus $m_{\text{x}}, m_{\text{y}} \approx 0$ according to (12.75). In other words, in the quasi-elastic regime, the total energy is almost completely dominated by the elastic energy [15, 16] and the energy transfer to the magnetic system during propagation can be neglected. On the other hand, in the quasi-magnetic regime, the dynamic displacement component u_{t} is very small and thus the total energy is dominated by the magnetic energy. In the magnetoelastic regime near the anticrossing, the total energy of the wave is distributed between the magnetic and elastic systems. Hence, a large part of the total wave energy resonantly oscillates between the magnetic and elastic domains [15, 16]. This is also seen in Fig. 12.3, which shows the magnetization components for the two branches of the dispersion relation, ω_+ and ω_-, as a function of the frequency. In keeping with the above discussion, the magnetization components have strong amplitudes in the quasi-magnetic and weak amplitudes in the quasi-elastic regime.

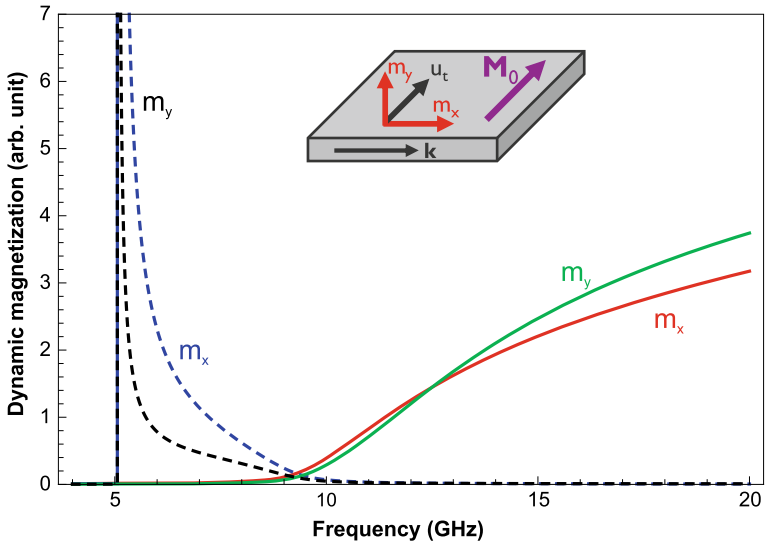

Fig. 12.3 Frequency dependence of the dynamic magnetization components of magnetoelastic waves in a 30 nm thick Ni film. The propagation direction is perpendicular to the magnetization, as shown in the inset. The dashed lines represent the m_x and m_y components of the ω_+ state, whereas the solid lines represent the m_x and m_y components of the ω_- state. The external magnetic field is $\mu_0 H_{ext} = 50\,\mathrm{mT}$

12.4.2.2 Wave Propagation Parallel to the Magnetization

When the propagation direction of the magnetoelastic wave is parallel to the equilibrium magnetization direction, i.e. $\theta = 0$ in (12.72), the magnetic body force $\mathbf{f}_{mel}$ acts on both the in-plane u_t and out-of-plane u_y transversal displacement components. Note that in this geometry, the transversal in-plane displacement component is fully aligned along the x-direction, i.e. $u_t = u_x$. Analogously, both the in-plane and the out-of-plane transversal elastic waves generate magnetoelastic fields that interact with the dynamic magnetization. Hence, both transversal displacement components couple to backward volume spin waves and only the longitudinal elastic wave is decoupled from the magnetic system. Neglecting longitudinal elastic waves, the system of equations in matrix notation becomes

$$\begin{bmatrix} \omega^2 - \omega_H^2 & 0 & \frac{iBk}{\rho M_s} & 0 \\ 0 & \omega^2 - \omega_V^2 & 0 & \frac{iBk}{\rho M_s} \\ i\gamma Bk & 0 & \omega_{fx} & -i\omega \\ 0 & i\gamma Bk & i\omega & \omega_{fy} \end{bmatrix} \begin{bmatrix} u_t \\ u_y \\ m_x \\ m_y \end{bmatrix} = 0\,. \tag{12.76}$$

It is worth noting that both transversal elastic waves have the same dispersion relation and thus $\omega_H = \omega_V = v_t k$, as discussed earlier.

Again, the homogeneous linear system has only nontrivial solutions when its determinant is zero. This condition leads to the dispersion relation of the resulting magnetoelastic waves, given by

$$(\omega^2-\omega_{\mathrm{fm}}^2)(\omega^2-\omega_{\mathrm{H}}^2)(\omega^2-\omega_{\mathrm{V}}^2)-Jk^2[\omega_{\mathrm{fx}}(\omega^2-\omega_{\mathrm{H}}^2)+\omega_{\mathrm{fy}}(\omega^2-\omega_{\mathrm{V}}^2)+Jk^2]=0\,. \tag{12.77}$$

Three different interaction terms can be identified in this equation. The first interaction term $Jk^2\omega_{\mathrm{fx}}(\omega^2-\omega_{\mathrm{H}}^2)$ represents the interaction between the out-of-plane u_{y} transversal elastic wave and the backward volume spin wave. The second term $Jk^2\omega_{\mathrm{fx}}(\omega^2-\omega_{\mathrm{V}}^2)$ characterizes the interaction between the in-plane u_{t} transversal elastic wave and the backward volume spin wave. As a result, these two terms induce an anticrossing near the point where the dispersion relations of the noninteracting elastic and magnetic waves would intersect each other. The third interaction term J^2k^4 couples all three different components with each other and thus also generates an interaction between the two transversal elastic waves.

Figure 12.4 shows the different dispersion relations for material parameters corresponding to Ni, as mentioned above. To better understand their behavior, the corresponding eigenstates of the different magnetoelastic waves are calculated. The eigenstates are given as a function of the angular frequency of the magnetoelastic wave, ω, by

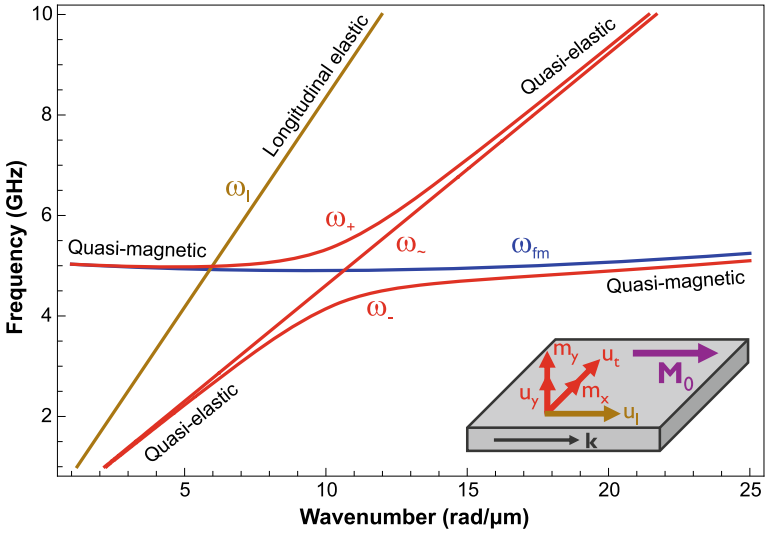

Fig. 12.4 Magnetoelastic wave dispersion relations (red lines) according to (12.77) for a 30 nm thick Ni film and propagation directions parallel with the magnetization, as shown in the inset. The external magnetic field is $\mu_0 H_{\mathrm{ext}} = 50\,\mathrm{mT}$. For comparison, the dispersion relations of longitudinal elastic waves (brown line) and uncoupled spin waves (blue line) are also shown

$$\begin{bmatrix} u_\mathrm{t} \\ u_\mathrm{y} \\ m_\mathrm{x} \\ m_\mathrm{y} \end{bmatrix} = N \begin{bmatrix} \frac{-i}{\omega(\omega^2-\omega_\mathrm{H}^2)}(\omega_\mathrm{fy}(\omega^2-\omega_\mathrm{V}^2)+Jk^2) \\ 1 \\ -\frac{\rho M_\mathrm{s}}{Bk\omega}(\omega_\mathrm{fy}(\omega^2-\omega_\mathrm{V}^2)+Jk^2) \\ i\frac{\rho M_\mathrm{s}}{Bk}(\omega^2-\omega_\mathrm{V}^2) \end{bmatrix} \tag{12.78}$$

with N a dimensionless normalization constant. The different displacement components of such magnetoelastic waves are plotted in Fig. 12.5 as a function of frequency, whereas Fig. 12.6 shows the magnetization components. As above, Ni material parameters were assumed, and the external magnetic field was $\mu_0 H_\mathrm{ext} = 50\,\mathrm{mT}$.

In the following, the different eigenstates and their properties are discussed. The upper ω_+ and lower ω_- branches of the dispersion relation both correspond to clockwise (right-hand) elliptically polarized waves for the magnetization and displacement, i.e. $m_\mathrm{y}/m_\mathrm{x} = i|m_\mathrm{y}|/|m_\mathrm{x}|$ and $u_\mathrm{y}/u_\mathrm{x} = i|u_\mathrm{y}|/|u_\mathrm{x}|$ [15, 16]. In both cases, the in-plane magnetization component is always larger than the out-of-plane component, i.e. $m_\mathrm{x} > m_\mathrm{y}$, since the demagnetization field is strongest in the out-of-plane direction. Concerning the displacement components, the two branches behave differently. For the ω_+ eigenstate, the in-plane and out-of-plane displacement components have the same order of magnitude at GHz frequencies. On the other hand, for the ω_- state,

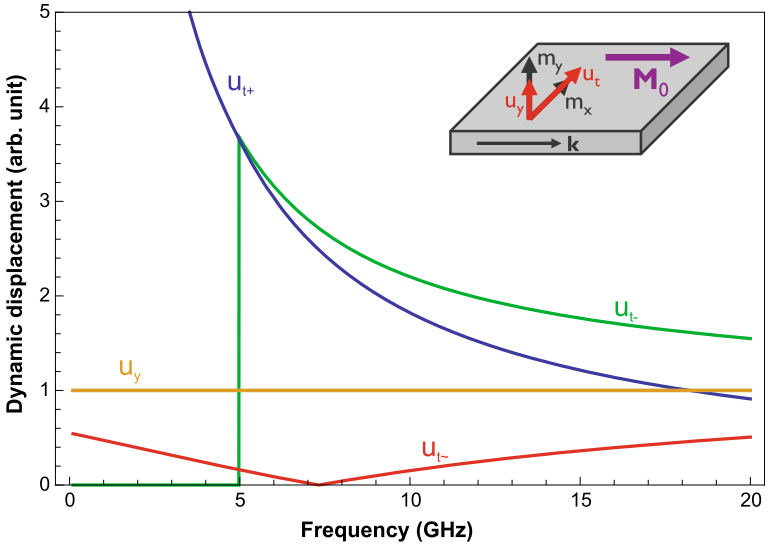

Fig. 12.5 Frequency dependence of the dynamic displacement components for the different magnetoelastic waves in a 30 nm thick Ni film and an external magnetic field of $\mu_0 H_\mathrm{ext} = 50\,\mathrm{mT}$. The propagation direction is parallel to the magnetization, as shown in the inset. All displacement values are normalized to the out-of-plane component of the displacement u_y (yellow line). The blue, green and red lines correspond to the in-plane displacement components of the ω_+, ω_- and $\omega_\sim$ modes, respectively

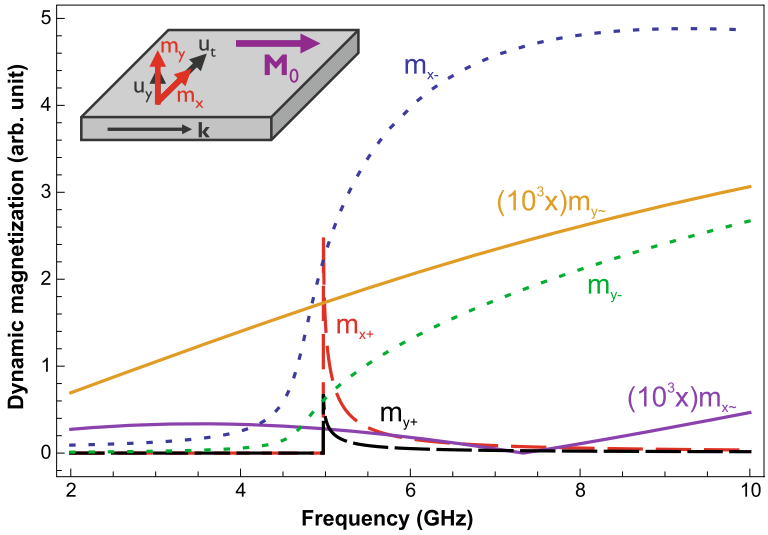

Fig. 12.6 Frequency dependence of the dynamic magnetization components of magnetoelastic waves in a 30 nm thick Ni film for an external magnetic field of $\mu_0 H_{\text{ext}} = 50\,\text{mT}$. The propagation direction is parallel to the magnetization, as shown in the inset. The dashed blue and green lines correspond to the ω_- mode, whereas the dashed red and black line correspond to the ω_+ modes, and the solid lines correspond to the $\omega_\sim$ mode. Note that the magnetization components corresponding to the $\omega_\sim$ mode are multiplied by a factor of 10^3

u_t is dominant at low frequencies, whereas u_y becomes dominant at high frequencies. This behavior is also visualized in Fig. 12.5.

The dispersion relation corresponding to the third magnetoelastic eigenstate is also shown in Fig. 12.4, labelled $\omega_\sim$. This dispersion relation is nearly linear and falls slightly below the dispersion relation for uncoupled transversal elastic waves, which was discussed in Sect. 12.3 [15, 16]. The magnetization and the displacement components corresponding to this state are both counterclockwise (left-hand) elliptically polarized. For uncoupled backward volume spin waves, counterclockwise polarization corresponds to evanescent spin waves. However, such evanescent spin waves can still couple to left-hand polarized displacement waves, resulting in left-hand polarized *propagating* magnetoelastic waves. Nonetheless, the magnetization components for this magnetoelastic mode remain very weak. This is also seen in Fig. 12.6, where the magnetization components corresponding to the $\omega_\sim$ branch have three orders of magnitude lower amplitude than the magnetization components of the ω_+ and ω_- branches. In terms of displacement, the u_y displacement component is dominant for the $\omega_\sim$ mode for a wide frequency range. This is also illustrated in Figs. 12.5 and 12.6.

Because of the coupling to the spin wave system, magnetoelastic waves show some peculiarities in the quasi-elastic regime, where the wave energy is largely dominated by the elastic energy. As shown above, the J^2k^4 interaction term couples all waves

with each other. Consequently, the two transversal elastic waves become also coupled. For interacting waves, it is impossible to share the same frequency–wavenumber couple, i.e. it is impossible to have degenerate points in the dispersion relations. As a result, the two quasi-elastic branches do not overlap anymore which is in contrast to their original behavior without magnetoelastic interactions (see Sect. 12.3). Therefore, at all frequencies, a small wavenumber shift remains present between the two quasi-elastic branches, even in the quasi-elastic regime where the displacement components are large and magnetization components are weak. Hence, even though almost all the wave energy is in the elastic system, the interaction between the two transversal displacement components is mediated by the magnetic system, leading to an indirect coupling of the two elastic waves via the magnetic system. This interaction is proportional to k^4 and thus strongly depends on the wavelength.

Moreover, the polarization of the displacement in the quasi-elastic regime also shows a peculiar behavior. One of the two waves in the quasi-elastic regime corresponds to a clockwise (right-hand) polarized wave and the other to a counterclockwise (left-hand) polarized wave, as discussed above. Hence, excitation at a single angular frequency ω in the quasi-elastic regime leads to two different magnetoelastic waves with different wavelengths and opposite polarization. Their amplitudes as a function of time and space can be written as

$$\mathbf{u}_{\pm} = \begin{bmatrix} |u_{\mathrm{t}\pm}| \\ i|u_{\mathrm{y}\pm}| \end{bmatrix} e^{i\omega t + k_{\pm} z} \quad \text{and} \quad \mathbf{u}_{\sim} = \begin{bmatrix} |u_{\mathrm{t}\sim}| \\ -i|u_{\mathrm{y}\sim}| \end{bmatrix} e^{i\omega t + k_{\sim} z} \tag{12.79}$$

with $u_{\mathrm{t}\pm} = u_{\mathrm{t}}(k_{\pm})$ and $u_{\mathrm{t}\sim} = u_{\mathrm{t}}(k_{\sim})$ given by (12.78). The total wave is the sum of both individual waves:

$$\mathbf{u}_{\mathrm{tot}} = \begin{bmatrix} |u_{\mathrm{t}\pm}| e^{ik_{\pm} z} + |u_{\mathrm{t}\sim}| e^{ik_{\sim} z} \\ i\left(|u_{\mathrm{y}\pm}| e^{ik_{\pm} z} - |u_{\mathrm{y}\sim}| e^{ik_{\sim} z}\right) \end{bmatrix} e^{i\omega t} \,. \tag{12.80}$$

The difference in amplitude between the clockwise and counterclockwise polarized components results in an elliptical polarization of the total displacement. The different wavenumbers of the two individual waves ($k_{\pm}$ and $k_{\sim}$) results in the rotation of the major and minor axes of the ellipsoid described by the tip of the displacement vectors during wave propagation [48, 49]. This is similar to the Faraday effect for electromagnetic waves and also called acoustic wave rotation.

The dispersion relation of backward volume spin waves is rather flat in the dipolar–exchange regime, leading to an interesting property of magnetoelastic waves in this geometry. As shown in Fig. 12.4 at frequencies around 4–5 GHz, the magnetoelastic coupling leads to the formation of a pseudobandgap for clockwise (right-hand) polarized elastic waves at the anticrossing. On the other hand, due to the flatness of the dispersion relation, counterclockwise (left-hand) polarized magnetoelastic waves can still exist in this pseudobandgap. Hence, in this frequency range, only pure magnetoelastic waves or quasi-magnetic waves with weak displacement components can be excited. This pseudobandgap formation is a general result when waves with a

rather flat dispersion relation interact with waves with a steep dispersion relation near the crossing point.

12.4.2.3 Arbitrary Propagation Direction

We now consider an arbitrary propagation direction of the magnetoelastic wave with respect to the equilibrium magnetization. In this case, the magnetoelastic body force interacts with all displacement components. Conversely, all displacement components generate magnetic fields that interact with the magnetization. Hence, all magnetization and displacement components become coupled with each other. Again, nontrivial wave-like solutions only exist when the determinant of the linear system in (12.68) is zero, which leads to the dispersion relation

$$\begin{aligned}&(\omega^2-\omega_l^2)[(\omega^2-\omega_{\mathrm{t}}^2)^2(\omega^2-\omega_{\mathrm{fm}}^2)\\ &-(\omega^2-\omega_{\mathrm{t}}^2)Jk^2(\omega_{\mathrm{fx}}\cos^2(\theta)+\omega_{\mathrm{fy}}\cos^2(2\theta))-J^2k^4\cos^2(2\theta)\cos^2(\theta)]\\ &-(\omega^2-\omega_{\mathrm{t}}^2)Jk^2[\omega_{\mathrm{fy}}(\omega^2-\omega_{\mathrm{t}}^2)\sin^2(2\theta)+Jk^2\sin^2(2\theta)\cos^2(\theta)]=0\,.\end{aligned} \tag{12.81}$$

Note that for $\theta=\pi/4$, the coupling between the magnetic and the longitudinal elastic wave reaches a maximum, whereas for $\theta=0$ and $\theta=\pi/2$, this coupling is zero.

The dispersion relations of the resulting magnetoelastic waves are plotted in Fig. 12.7 for material parameters of Ni and $\theta=\pi/6$. For each frequency, multiple magnetoelastic waves exist with different wavelengths. Since the system of equations is reduced to a set of linear differential equations by assuming weak dynamic components, every linear combination of these different magnetoelastic waves is also a solution of the system. The waves can be excited by dynamic magnetic fields and/or mechanical forces. Therefore, it is possible to generate elastodynamics via the magnetization or, vice versa, magnetization dynamics via the displacement in magnetostrictive materials.

It can also be seen from the dispersion relations that the group velocity of the magnetoelastic waves is different from the group velocity of the magnetic and elastic waves. As mentioned earlier, the group velocity is defined as $\mathbf{v}_{\mathrm{g}}=\partial\omega/\partial\mathbf{k}$ and thus proportional to the slope of the dispersion relation. Hence, near the anticrossing, this change in group velocity is most pronounced. On the other hand, the group velocity of quasi-elastic and quasi-magnetic waves is nearly the same as their purely elastic and magnetic counterparts, respectively.

The total energy of a magnetoelastic wave consists of several contributions. The magnetic energy contribution is determined by the dynamic components m_{x} and m_{y}. In this chapter, only dipolar, and exchange energy interactions were considered, although other magnetic interactions, such as the magnetocrystalline [40, 41, 50] or the Dzyaloshinskii–Moriya interaction [51] may also contribute to the total energy. The magnetic energy is complemented by the energy of the elastic waves, which consists of both elastic and kinetic energy contributions and is fully determined by the

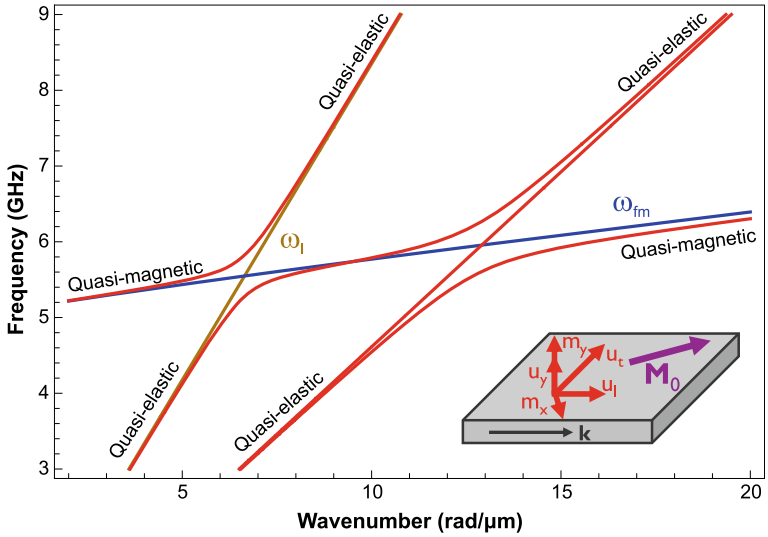

Fig. 12.7 Magnetoelastic wave dispersion relations (red lines) according to (12.81) for a 30 nm thick Ni film nm and an angle of 30° between the propagation direction and the magnetization. The external field is $\mu_0 H_{\text{ext}} = 50\,\text{mT}$. For comparison, the dispersion relations of longitudinal elastic waves (brown line) and uncoupled spin waves (blue line) are also shown

displacement components and their time and space derivatives, as given by (12.54) and (12.56), respectively. A third energy contribution stems from the magnetoelastic interaction, as described by (12.57). Just as spin waves (cf. (12.41)), magnetoelastic waves also comprise an electric field component. However, at GHz frequencies, the magnetostatic approximation is typically valid and therefore the energy contribution of the electric field is small and can be neglected. Nonetheless, this ceases to be accurate when frequencies approach the THz range where the magnetostatic approximation no longer holds.

During the propagation of a magnetoelastic wave, the energy oscillates between the different energy contributions. For strongly interacting waves near the anticrossing point, a large part of the energy resonantly oscillates between the elastic and magnetic domains. This energy transfer is characterized by a specific energy transfer length L_t which describes the distance necessary to transfer all energy from the elastic to the magnetic system and vice versa [52]. On the other hand, the time necessary for a complete magnetoelastic energy oscillation between the elastic and magnetic domain is given by $\Gamma = 2/\Delta f$ with Δf the frequency gap between the two dispersion relations (cf. (12.73)) [53]. By contrast, in the quasi-elastic regime, most of the energy remains in the elastic system during propagation, whereas in the quasi-magnetic regime most energy remains in the magnetic system [15, 16].

In this chapter, it was assumed that the wavelength of the magnetoelastic wave is much larger than the thickness of the film. In this case, the dynamic magnetization and displacement are approximately uniform over the film thickness. However, if

the thickness becomes comparable to the wavelength, different thickness modes can arise. In the magnetic domain, these are called perpendicularly standing spin waves and in the elasticity domain, these are called Lamb waves. The magnetoelastic coupling of such waves is beyond the scope of this chapter and will generally require numerical calculations.

12.4.3 Damping of Magnetoelastic Waves

So far, all waves have been considered to be lossless and their intrinsic damping was neglected. However, in real systems, magnetoelastic waves are expected to decay during propagation. Since their decay length is of great practical interest, we will present in this last part a brief introduction on the damping of magnetoelastic waves. More detailed discussions can be found in [54–58].

Several different energy loss mechanisms exist, which dampen the magnetization and displacement dynamics. In the semi-classical continuum theory used in this chapter, it is common to subsume all different loss mechanisms in a single phenomenological damping term, which is then included in the equation of motion. The damping of the magnetization dynamics is captured by the damping term in the LLG equation, characterized by the phenomenological Gilbert damping parameter α. Analogously, for elastic waves, damping can be introduced into the equations of motion via phenomenological complex stiffness constants.

The addition of the damping terms to the equations of motion results in energy dissipation of the dynamic system. As a consequence, the amplitude of the plane waves considered above decays in time and space. Therefore, the plane wave ansatz to solve the equations of motion needs to be modified by adding an exponential decay factor. This damping factor can be seen as originating from the complex frequency, i.e.

$$\mathbf{w}(\mathbf{r},t)e^{i((\omega_r+i\omega_i)t+\mathbf{k}\cdot\mathbf{r})} = \mathbf{w}(\mathbf{r},t)e^{-t/\tau}e^{i(\omega_r t+\mathbf{k}\cdot\mathbf{r})} = \mathbf{w}(\mathbf{r},t)e^{-x/\delta}e^{i(\omega_r t+\mathbf{k}\cdot\mathbf{r})} \quad (12.82)$$

with $\tau = 1/\omega_i$ the lifetime, $\delta = v_g\tau$ the mean free path or attenuation length, and $\mathbf{w}(\mathbf{r},t) = [u_\mathrm{x}, u_\mathrm{y}, u_\mathrm{z}, m_\mathrm{x}, m_\mathrm{y}]^T$ the dynamic components of the wave. Note that the lifetime characterizes the decay of the wave in time and the mean free path characterizes the attenuation of the wave in space.

To determine the decay characteristics of a wave, the imaginary part of its frequency needs to be assessed. This can be achieved within the above approach, which is based on finding nontrivial solutions of homogeneous linear systems by calculating the roots of their determinants. The real part of the resulting frequency still represents the dispersion relation, whereas the imaginary part originates from the additional damping terms and represents the inverse of the lifetime.

For spin waves in a ferromagnetic medium, the lifetime can be found by solving the LLG equation and is given by

$$\tau_{\mathrm{fm}} = \frac{2}{\alpha(\omega_{\mathrm{fx}} + \omega_{\mathrm{fy}})} . \tag{12.83}$$

The lifetime at GHz frequencies is typically of the order of ns in metallic ferromagnets, such as Ni considered in this chapter, and of the order of μs for low-damping magnetic insulators such as Yttrium Iron Garnet (YIG). On the other hand, much less is know for elastic waves at GHz frequencies although estimates suggest that the lifetime is similar to that of spin waves. Experimentally, it is typically found that the mean free path of (surface) elastic waves at these frequencies is somewhat larger than these of spin waves [40, 51, 52, 59], however, the topic still requires further research.

In the case of magnetoelastic waves, analytical derivations of the lifetimes and decay lengths are rather complex. In the quasi-elastic regime, it is clear that the lifetime is strongly determined by the lifetime of the elastic wave. The energy of quasi-elastic waves is almost completely stored in the elastic system, with only a negligible part in the magnetic system. Hence, the dissipation due to the magnetic loss has negligible influence on the overall dissipation. An analogous argument can be made for the quasi-magnetic regime, where magnetic properties and lifetimes should determine the decay of the magnetoelastic waves.

In the strongly coupled magnetoelastic regime, i.e. near the anticrossing, no simple conclusion can be drawn. In this regime, the energy is distributed between magnetic and elastic domains and is transferred forth and back during propagation. Therefore both magnetic and elastic losses contribute to the total energy dissipation. One may expect in such a case that the lifetime of a magnetoelastic wave is given by a suitable weighted average of the lifetimes of magnetic and elastic waves. In general, the lifetime depends on multiple parameters, such as the orientation of the static magnetization, the interaction coefficient, the wavenumber, etc.. Further work is required to fully understand in particular the effect of the magnetoelastic interactions on the lifetime of strongly coupled magnetoelastic waves. By contrast, the group velocities of magnetoelastic waves are well understood and can be calculated from the dispersion relations, so the assessment of mean free paths is straighforward once the lifetime is known.

12.5 Conclusion

The first part of this chapter presented a review of magnetic and elastic interactions as well as the formation of magnetic (spin) and elastic waves. It has been shown that the dynamic behavior of the magnetization and displacement can be seen as an eigensystem with eigenvalues corresponding to the dispersion relations and eigenstates describing the polarization and ellipticity of the resulting waves. Based on this formalism of eigensystems, both magnetic and elastic waves have been studied in bulk and thin film materials. For magnetic (spin) waves, different regimes have been identified and their correlation with Maxwell's equations has been explained.

In the second part of this chapter, the coupling between magnetic and elastic waves, due to the direct and inverse magnetoelastic interactions, was described. By combining the magnetoelastic interaction terms with the magnetodynamic and the elastodynamic equations, the magnetoelastic eigensystem has been derived for an arbitrary in-plane magnetization orientation. Within this framework, both the exchange and dipolar interaction have been taken into account. Previous descriptions of magnetoelastic waves in infinitesimally thin films have been extended to thin films of finite thickness by considering the appropriate dipolar field based on the magnetostatic Green's function. Two limiting cases, i.e. static magnetization perpendicular or parallel to the propagation direction, have been studied in more detail and their dispersion relations and eigenstates have been mathematically and graphically described. In addition, several properties of magnetoelastic waves, such as the energy transfer length and the magnetoelastic bandgap, and concepts, such as wave anticrossings and polarization rotations, have been discussed in detail. The fundamental framework of magnetoelastic phenomena and waves described in this chapter can be utilised for the theoretical description and modeling of the next generation of magnetoelectric transducers. These transducers need to operate at GHz frequencies and should be miniaturized to the nanometer scale. Despite the technical challenges, such transducers show high potential for efficient energy transfer between the electric and magnetic domains.

Acknowledgements This work has been supported by imec's industrial affiliate program on beyond-CMOS logic and by the European Union's Horizon 2020 research and innovation program within the FET-OPEN project CHIRON under grant agreement No. 801055. F.V. acknowledges financial support from the Research Foundation – Flanders (FWO) through grant No. 1S05719N.

References

1. Z. Diao, Z. Li, S. Wang, Y. Ding, A. Panchula, E. Chen, L. Wang, Y. Huai, Spin-transfer torque switching in magnetic tunnel junctions and spin-transfer torque random access memory. J. Phys.-Condens. Matter **19**, 165209 (2007)
2. M. Bapna, B. Parks, S.D. Oberdick, H. Almasi, W. Wang, S.A. Majetich, Spin-orbit-torque switching in 20-nm perpendicular magnetic tunnel junctions. Phys. Rev. Appl. **10**, 024013 (2018)
3. N.I. Polzikovaa, S.G. Alekseev, I.I. Pyataikin, I.M. Kotelyanskii, V.A. Luzanov, A.P. Orlov, Acoustic spin pumping in magnetoelectric bulk acoustic wave resonator. AIP Adv. **6**, 056306 (2016)
4. S. Cherepov, P.K. Amiri, J.G. Alzate, K. Wong, M. Lewis, P. Upadhyaya, J. Nath, M. Bao, A. Bur, T. Wu, G.P. Carman, A. Khitun, K.L. Wang, Electric-field-induced spin wave generation using multiferroic magnetoelectric cells. Appl. Phys. Lett. **104**, 082403 (2014)
5. N.I. Polzikova, S.G. Alekseev, V.A. Luzanov, A.O. Raevskiy, Electroacoustic excitation of spin waves and their detection due to the inverse spin hall effect. Phys. Solid State **60**, 2211–2217 (2018)
6. M. Balinskiy, A.C. Chavez, A. Barra, H. Chiang, G.P. Carman, A. Khitun, Magnetoelectric spin wave modulator based on synthetic multiferroic structure. Sci. Rep. **8**, 10867 (2018)
7. H. Zhou, A. Talbi, N. Tiercelin, O. Bou Matar, Multilayer magnetostrictive structure based surface acoustic wave devices. Appl. Phys. Lett. **104**, 114101 (2014)

8. C. Kittel, Interaction of spin waves and ultrasonic waves in ferromagnetic crystals. Phys. Rev. **110**, 836 (1958)
9. A.I. Akhiezer, V.G. Bar'iakhtar, S.V. Peletminskii, Coupled magnetoelastic waves in ferromagnetic media and ferroacoustic resonance. JETP **8**, 157 (1959)
10. P.A. Fedders, Theory of acoustic resonance and dispersion in bulk ferromagnets. Phys. Rev. B **9**, 3835 (1974)
11. T. Kobayashi, R.C. Barker, J.L. Bleustein, A. Yelon, Ferromagnetoelastic resonance in thin films I. Formal treatment. Phys. Rev. B **7**, 3273 (1973)
12. T. Kobayashi, R.C. Barker, A. Yelon, Ferromagnetoelastic resonance in thin films. II. Application to nickel. Phys. Rev. B **7**, 3286 (1973)
13. A. Kamra, G.E.W. Bauer, Actuation, propagation, and detection of transverse magnetoelastic waves in ferromagnets. Solid State Commun. **198**, 35–39 (2014)
14. S.M. Keller, A. Sepulveda, G.P. Carman, Effective magnetoelectric properties of magnetoelectroelastic (multiferroic) materials and effects on plane wave dynamics. Prog. Electromagn. Res. **154**, 115–126 (2015)
15. V.W. Tucker, J.W. Rampton, *Microwave Ultrasonics in Solid State Physics* (North Holland, 1972)
16. A.G. Gurevich, G.A. Melkov, *Magnetization Oscillations and Waves* (CRC Press, 1996)
17. E. Schlomann, Generation of phonons in high power ferromagnetic resonance experiments. J. Appl. Phys. **31**, 1647 (1960)
18. L. Landau, E. Lifshitz, On the theory of the dispersion of magnetic permeability in ferromagnetic bodies. Phys. Z. Sowjetunion **8**, 153–164 (1935)
19. T.L. Gilbert, A phenomenological theory of damping in ferromagnetic materials. IEEE Trans. Magn. **40**, 3443 (2004)
20. D.D. Stancil, A. Prabhakar, *Spin Waves Theory and Applications* (Springer, 2009)
21. M.G. Cottam, *Linear and Nonlinear Spin Waves in Magnetic Films and Superlattices* (World Scientific Publishing Company, 1994)
22. R.I. Joseph, E. Schlömann, Demagnetizing field in nonellipsoidal bodies. J. Appl. Phys. **36**, 1579 (1965)
23. A. Smith, K.K. Nielsen, D.V. Christensen, C.R.H. Bahl, R. Bjork, J. Hattel, The demagnetizing field of a nonuniform rectangular prism. J. Appl. Phys. **107**, 103910 (2010)
24. S. Chikazumi, *Physics of Magnetism* (Krieger Pub Co, 1986)
25. B. Hillebrands, K. Ounadjela, *Spin Dynamics in Confined Magnetic Structures I* (Springer, 2002)
26. C. Herring, C. Kittel, On the theory of spin waves in ferromagnetic media. Phys. Rev. **81**, 869 (1951)
27. S. Tamaru, J.A. Bain, M.H. Kryder, D.S. Ricketts, Green's function for magnetostatic surface waves and its application to the study of diffraction patterns. Phys. Rev. B **84**, 064437 (2011)
28. R.W. Damon, J.R. Eshbach, Magnetostatic modes of a ferromagnet slab. J. Phys. Chem. Solids **19**, 308–320 (1961)
29. K.J. Harte, Theory of magnetization ripple in ferromagnetic films. J. Appl. Phys. **39**, 1503 (1968)
30. B.A. Kalinikos, A.N. Slavin, Theory of dipole-exchange spin wave spectrum for ferromagnetic films with mixed exchange boundary conditions. J. Phys. C: Solid State Phys. **19**, 7013–7033 (1986)
31. B.A. Kalinikos, Spectrum and linear excitation of spin waves in ferromagnetic films. Sov. Phys. J. **24**, 718–731 (1981)
32. B.D. Cullity, C.D. Graham, *Introduction to Magnetic Materials* (Wiley, 2011)
33. C. Wilts, S. Lai, Spin wave measurements of exchange constant in Ni-Fe alloy films. IEEE Trans. Magn. **8**, 280 (1972)
34. M. Ewing, *Elastic Waves in Layered Media*. McGraw-Hill Series in the Geological Sciences (1957)
35. J.R. Barber, *Elasticity* (Kluwer Academic Publishers, 2004)
36. K.F. Graff, *Wave Motion in Elastic Solids* (Dover Publications, 1975)

37. J. D. Achenbach, *Wave Propagating in Elastic Solids* (North-Holland Publishing, 1973)
38. A.H. Nayfeh, *Wave Propagation in Layered Anisotropic Media* (North-Holland Publishing, 1995)
39. A.K. Ganguly, K.L. Davis, D.C. Webb, C. Vittoria, Magnetoelastic surface waves in a magnetic film-piezoelectric substrate configuration. J. Appl. Phys. **47**, 2696 (1976)
40. L. Dreher, M. Weiler, M. Pernpeintner, H. Huebl, R. Gross, M.S. Brandt, S.T.B. Goennenwein, Surface acoustic wave driven ferromagnetic resonance in nickel thin films: theory and experiment. Phys. Rev. B **86**, 134415 (2012)
41. L. Thevenard, C. Gourdon, J.Y. Prieur, H.J. von Bardeleben, S. Vincent, L. Becerra, L. Largeau, J.-Y. Duquesne, Surface-acoustic-wave-driven ferromagnetic resonance in (Ga, Mn)(As, P) epilayers. Phys. Rev. B **90**, 094401 (2014)
42. E. du Tremolet, de Lacheisseirie, *Magnetostriction—Theory and Applications of Magnetoelasticity* (CRC Press, Boca Raton, 1993)
43. R.C. O'Handley, *Modern Magnetic Materials: Principles and Applications* (John Wiley & Sons, Inc., 2000)
44. J. Walowski, M. Djordjevic Kaufmann, B. Lenk, C. Hamann, J. McCord, M. Münzenberg, Intrinsic and non-local Gilbert damping in polycrystalline nickel studied by Ti: sapphire laser fs spectroscopy. J. Phys. D **41**, 164016 (2008)
45. D. Sander, The correlation between mechanical stress and magnetic anisotropy in ultrathin films. Rep. Prog. Phys. **62**, 809 (1999)
46. M. Yamamoto, On elastic constants of nickel crystals. Phys. Rev. **77**, 566 (1950)
47. A.F. Mills, *Basic Heat and Mass Transfer*, 2nd edn. (Prentice Hall, New Jersey, 1999)
48. H. Matthews, R.C. Le Craw, Acoustic wave rotation by magnon-phonon interaction. Phys. Rev. Lett. **8**, 397 (1962)
49. K.B. Vlasov, B.K. Ishmukhametov, Rotation of the plane of polarization of elastic waves in magnetically polarized magneto-elastic media. Sov. Phys. JETP **10**, 531 (1960)
50. P.G. Gowtham, T. Moriyama, D.C. Ralph, R.A. Buhrman, Travelling surface spin-wave resonance spectroscopy using surface acoustic waves. J. Appl. Phys. **118**, 233910 (2015)
51. R. Verba, I. Lisenkov, I. Krivorotov, V. Tiberkevich, A. Slavin, Nonreciprocal surface acoustic waves in multilayers with magnetoelastic and interfacial Dzyaloshinskii-Moriya interactions. Phys. Rev. Appl. **9**, 064014 (2018)
52. P. Graczyk, M. Krawczyk, Coupled-mode theory for the interaction between acoustic waves and spin waves in magnonic-phononic crystals: Propagating magnetoelastic waves. Phys. Rev. B **96**, 024407 (2017)
53. C. Berk, M. Jaris, W. Yang, S. Dhuey, S. Cabrini, H. Schmidt, Strongly coupled magnon-phonon dynamics in a single nanomagnet. Nat. Commun. **10**, 2652 (2019)
54. S.M. Rezende, F.R. Morgenthaler, Magnetoelastic waves in time-varying magnetic fields. I. Theory. J. Appl. Phys. **40**, 524 (1969)
55. A. Widom, C. Vittoria, S.D. Yoon, Gilbert ferromagnetic damping theory and the fluctuation-dissipation theorem. J. Appl. Phys. **108**, 073924 (2010)
56. V.L. Gurevich, Dissipation function in a magnetic field (Review). Phys. Solid State **57**, 1271–1276 (2015)
57. E. Rossi, O.G. Heinonen, A.H. MacDonald, Dynamics of magnetization coupled to a thermal bath of elastic modes. Phys. Rev. B **72**, 174412 (2005)
58. S. Streib, H. Keshtgar, G. Bauer, Damping of magnetization dynamics by phonon pumping. Phys. Rev. Lett. **121**, 027202 (2018)
59. X. Li, D. Labanowski, S. Salahuddin, C.S. Lynch, Spin wave generation by surface acoustic waves. J. Appl. Phys. **122**, 043904 (2017)